Pregnancy Reduces COVID-19 Vaccine Immunity Against Novel Variants

Maclaine A. Parish[1], Jaiprasath Sachithanandham[1], Lizeth Gutierrez[2], Han-Sol Park[1], Anna Yin[1], Katerina Roznik[2], Patrick Creisher[1], John S. Lee[1], Laura A. St Clair, [1] Annie Werner[1], Susan Bersoff-Matcha[3], Catherine Pilgrim-Grayson[4], Lea Berhane[4], Hana Golding[5], Patrick Shea[1], Katherine Fenstermacher[6], Richard Rothman[6], Irina Burd[7], Jeanne Sheffield[8], Andrea L. Cox[1,2], Andrew Pekosz[1,2,6], and Sabra L. Klein[1,2*]

[1]W. Harry Feinstone Department of Molecular Microbiology and Immunology, Johns Hopkins University Bloomberg School of Public Health, Baltimore, MD, USA

[2]Department of Medicine, Division of Infectious Diseases, Johns Hopkins School of Medicine, Baltimore, MD, USA

[3]Office of Women's Health, U.S. Food and Drug Administration, Silver Spring, MD, USA

[4]Division of Urology, Obstetrics, and Gynecology; Office of Rare Diseases, Pediatrics, Urologic and Reproductive Medicine; Office of New Drugs; Center for Drug Evaluation and Research; U.S. Food and Drug Administration, Silver Spring, MD, USA

[5]Division of Viral Products, Center of Biologics Evaluation and Research, U.S. Food and Drug Administration, Silver Spring, MD, USA

[6]Department of Emergency Medicine, Johns Hopkins School of Medicine, Baltimore, MD, USA

[7]Department of Obstetrics, Gynecology and Reproductive Sciences, University of Maryland School of Medicine, Baltimore, MD, USA

[8]Department of Obstetrics and Gynecology, Johns Hopkins School of Medicine, Baltimore, MD, USA

*Address correspondence to Sabra L. Klein, (410)955-8898, sklein2@jhu.edu

Abstract

Pregnant women are at heightened risk for severe outcomes from many infectious diseases, including COVID-19. However, they were not included in the initial COVID-19 vaccine clinical trials and current rates of vaccine uptake among pregnant women remain below 15%. We explored the serological and cellular responses to COVID-19 mRNA booster vaccines (i.e., ancestral and BA.5) in pregnant and age-matched non-pregnant females to identify how pregnancy affects immunity against vaccine viruses in addition to novel variants. Blood was collected from participants prior to and 3-5 weeks post booster vaccine. Post-vaccination antibodies from pregnant women were less cross-reactive to non-vaccine antigens, including XBB1.5 and JN.1, than antibodies from non-pregnant females. Antibodies from non-pregnant females showed strong correlations between IgG1 and FcR binding and greater IgG1:IgG3 ratios and live virus neutralization against all variants. In contrast, antibodies from pregnant women had lower IgG1:IgG3 ratios and neutralization and greater antibody-dependent NK cell cytokine production and neutrophil phagocytosis, particularly against variants. CD4+ T cells from pregnant patients exhibited reduced polyfunctionality, with IFNγ+ monofunctional dominance. In contrast, among non-pregnant women, CD4+ T cells displayed greater polyfunctionality, with more IL-21+ cells. Pregnancy may reduce the breadth, composition, and magnitude of humoral and cellular immunity, particularly in response to novel variants.

44 **Introduction**

45 Pregnant women faced significant morbidity and mortality during the COVID-19
46 pandemic, with an elevated risk for severe outcomes [1-3]. From the onset of the pandemic
47 in early 2020 to December 2022, there were 24,203 cases of COVID-19 among pregnant
48 women in the United States with 2,043 fatalities [4]. This 8.4% mortality rate is significantly
49 higher than that of the general population (0.061%), reflecting the elevated risk for disease
50 outcomes in pregnancy. Pregnant women also were more likely to require hospitalization
51 and invasive ventilation from acute SARS-CoV-2 infection than non-pregnant women [3, 4].
52 Adverse pregnancy outcomes were an additional concern as SARS-CoV-2 infection has
53 been associated with preeclampsia, stillbirth, NICU admission, and preterm birth in
54 women [1, 5, 6] and mouse models [7].

55 The Centers for Disease Control and Prevention (CDC) and the American College of
56 Obstetricians and Gynecologists (ACOG) recommend vaccination during pregnancy to
57 provide optimal protection against SARS-CoV-2 for both the mother and fetus [8]. Data
58 from November 2021 show vaccination rates among pregnant women (45.1%) were
59 significantly lower than that of non-pregnant people (64.9%) [9]. Vaccination rates among
60 pregnant women have since fallen precipitously, and remain lower than non-pregnant
61 people, with less than 15% of pregnant women vaccinated in the 2023-2024 vaccination
62 season [10]. This decline in vaccine uptake is particularly concerning given that other
63 vaccines offered during pregnancy, such as influenza and Tdap, show higher coverage rates
64 (47.4% and 59.6%, respectively) [10, 11]. Despite proven safety of COVID-19 vaccines

65 during pregnancy [12], low vaccine uptake may be a result of greater vaccine hesitancy in
66 this population [13-15] (Parish et al., 2025b, submitted).

67 While vaccination is the best preventative strategy to reduce the severity of COVID-
68 19 outcomes [12, 16], existing evidence suggest pregnant women mount dampened
69 immune responses to vaccination, highlighting the need for deeper immunological
70 assessments [17]. Previous studies of COVID-19 vaccines in pregnant women have
71 focused on placental antibody transfer following vaccination during pregnancy,
72 demonstrating the benefits of maternal vaccination in protecting newborns and infants
73 from severe infection [18-20]. While several studies have aimed to compare the antibody
74 landscape induced by vaccination during pregnancy to those in non-pregnant women [21],
75 to date, the effects of pregnancy on cross-protection against circulating variants in addition
76 to vaccine antigens has remained unexplored.

77 Using systems serology, we can broadly and deeply characterize the antibody
78 landscape in response to COVID-19 vaccination. By employing this systematic and
79 comprehensive approach, we can gain insight to shape future vaccine development and
80 public health campaigns by understanding the protective immune response generated by
81 vaccination [22]. Combining functional assays and systems serology methods, we show
82 that the breadth and diversity of antibody generated by vaccination and polyfunctionality of
83 spike-specific memory CD4+ T cells are reduced during pregnancy.

84

85 **Methods**

86 ***Study Design***

87 Pregnant women were enrolled into mRNA vaccine studies at the Johns Hopkins Maternal
88 & Fetal Medicine Clinic (IRB 00246472) (n=7 pregnant) during the 2022-2023 vaccination
89 season. Pregnant women were contacted at clinical visits or via phone to determine
90 interest and eligibility. Women were eligible if they planned to receive an mRNA COVID
91 booster vaccine (Pfizer of Moderna) during weeks 32 through 36 of pregnancy, and consent
92 to maternal blood collection before and after receipt of the booster vaccine. Patients who
93 had already received an initial dose(s) of the vaccine were still eligible to enroll. Throughout
94 recruitment, 232 pregnant women were approached to participate in this study. Ninety-one
95 patients were initially interested while only 14 enrolled in the study. Of these, 7 completed
96 the study. For non-pregnant female comparators, samples were obtained from age-
97 matched adult female healthcare workers who were recruited during the 2022-2023
98 influenza vaccine enrollment period by fliers, emails, and announcements about the
99 annual vaccination program and were able to self-enroll upon receipt of the influenza
100 vaccine at the Johns Hopkins East Baltimore hospital (IRB00288258) (n = 13 non-pregnant).
101 Demographic information is detailed in **Table 1**. Of the vaccinees enrolled, 13 age-matched
102 non-pregnant females received the COVID-19 booster vaccine during the same vaccination
103 season and had pre- and post-vaccination blood samples available. Plasma and peripheral
104 blood mononuclear cells were obtained prior to and one month after receipt of mRNA
105 booster vaccines from pregnant and non-pregnant females. Plasma was used to assess
106 antigen-specific immunoglobulin isotype responses and live virus neutralizing antibody
107 responses, in addition to the crystallizable fragment (Fc) receptor affinity and non-

108 neutralizing antibody functions. Cryopreserved PBMCs were used for flow cytometry
109 analyses.

110 ***Cells and Viruses***

111 Vero-E6-TMPRSS2 cells were obtained from the cell repository of the National
112 Institute of Infectious Diseases, Japan and were grown in complete media consisting of
113 Dulbecco's modified eagle medium (DMEM) (Gibco, Thermo Fisher Scientific), containing
114 10% fetal bovine serum (FBS) (Gibco, Thermo Fisher Scientific), 1 mM glutamine
115 (Invitrogen, Thermo Fisher Scientific), 1 mM sodium pyruvate (Invitrogen, Thermo Fisher
116 Scientific), 100 U/mL penicillin (Invitrogen, Thermo Fisher Scientific), and 100 µg/mL
117 streptomycin (Invitrogen, Thermo Fisher Scientific). Cells were incubated at 37°C in a
118 humidified incubator with 5% CO2.

119 Ancestral (hCoV-19/USA/DC-HP00007/2020; B.1, GISAID EPI_ISL_434688), BA.5
120 (hCoV-19/USA/MD-HP32103-PIDCNSQVGY/2022, GISAID EPI_ISL_15013106), XBB.1.5
121 (hCoV-19/USA/MD-HP40900-PIDYSWHNUB/2022, GISAID EPI_ISL_16026423), and JN.1
122 (hCoV-19/USA/MD-HP49672-PIDDVSVURS/2023, GISAID EPI_ISL_18623285) variants of
123 SARS-CoV-2 were isolated from Vero-E6-TMPRSS2 cells plated in 24-well plates as
124 previously described [23]. The consensus sequence of the virus isolate did not differ from
125 the sequence derived from the clinical specimen. The infectious virus titer was determined
126 on Vero-TMPRSS2 cells using a 50% tissue culture infectious dose (TCID50) assay as
127 described [24].

128 ***Microneutralization assays***

129 Plasma neutralizing antibodies [25] were determined as described for SARS-CoV
130 and modified for SARS-CoV-2 as described [26]. Two- fold dilutions of plasma, starting at a
131 1:20 dilution, were made using incomplete media (IM) - Dulbecco's modified eagle medium
132 (DMEM) (Gibco, Thermo Fisher Scientific), containing 1 mM glutamine (Invitrogen, Thermo
133 Fisher Scientific), 1 mM sodium pyruvate (Invitrogen, Thermo Fisher Scientific), 100 U/mL
134 penicillin (Invitrogen, Thermo Fisher Scientific), and 100 µg/mL streptomycin (Invitrogen,
135 Thermo Fisher Scientific). Infectious virus was added to the plasma dilutions at a final
136 concentration of 1 × 10^3 TCID50/mL or 100 TCID50 per 100 µL. The plasma-virus solution
137 was incubated at room temperature for 1 hour, and 100 µL of each dilution was added to 1
138 well of a 96-well plate of VeroE6-TMPRSS2 cells in hextuplicate. The cells were incubated
139 for 6 hours at 37°C with 5% CO2. The inoculum was replaced with fresh IM, and the cells
140 were incubated at 37°C with 5% CO2 for 3-4 days until cytopathic effect (CPE) is evident in
141 the no serum controls. The cells were fixed by the addition of 100 µL of 4% formaldehyde
142 for at least 4 hours at room temperature, and then stained with naphthol blue-black
143 overnight. The nAb titer was calculated as the highest serum dilution that eliminated the
144 CPE in 50% of the wells (NT50) and the AUC was calculated [27, 28].

145 ***Antigen-bead coupling***

146 Antigen-specific isotyping and Fc receptor binding affinity were multiplexed using a
147 Luminex Intelliflex in a 384-well format. Antigens used in this panel are as follows:
148 ancestral spike (S) and nucleocapsid (N) protein, BA.5, XBB.1.5, and JN.1 spike proteins
149 were obtained through the National Cancer Institute Serological Sciences Networks
150 (SeroNet) for COVID-19 [29]. Each antigen was coupled to unique bead MagPlex bead

151 regions (Luminex). Briefly, beads were activated by activation solution consisting of
152 activation buffer (0.1M NaH2PO4; pH 6.2), 50mg/mL 1-ethyl-3-[3-dimethylaminopropyl]
153 carbodiimide (EDC), and 50mg/mL Sulfo-NHS (N-hydroxysulfosuccinimide). Activated
154 beads were coupled to 25ug of antigen in coupling buffer (0.05M MES; pH 5.0). Activated
155 coupled beads were blocked with blocking buffer (PBS 1X, 0.1%BSA, 0.02% Tween-20,
156 0.05% Sodium azide; pH 7.4), washed with washing buffer (PBS 1X, 0.05% Tween-20) and
157 stored at 4C in PBS.

158 ***Luminex serological assays***

159 Serum was diluted 1:25 and was incubated with bead solution (20uL of each bead
160 region in 20mL of Luminex Assay Buffer - PBS 1X, 0.1% BSA, 0.05% Tween). This protocol
161 was followed for isotyping (IgM, IgG [IgG1-4], and IgA [IgA1-2]) and binding to the following
162 Fc receptors (FcRs): FcγRIIA-R, FcγRIIA-H, FcγRIIb, FcγRIIIA-V, FcγRIIIA-F, FcγRIIIB, FcRn,
163 and FcαR (Duke Vaccine Institute – Protein Production facility). Following incubation,
164 plates were placed on a magnet and washed with Procartaplex Wash Buffer
165 (ThermoFisher). Each assay plate was then incubated with 45uL of secondary antibody
166 diluted in Luminex Assay Buffer. Isotypes were identified by PE-conjugated antibodies
167 (Southern Biotech) and FcR proteins were biotinylated using BirA biotin-ligation kit (Avidity)
168 at least one day prior and coupled to PE-Streptavidin (BioLegend). Following incubation
169 with secondary antibody, plates were placed on a magnet and washed. Beads were
170 resuspended in Procartaplex Wash Buffer before running on the Luminex Intelliflex.
171 Samples were run on FlexMap 3D Low with a DD range of 7000-1700. For each assay, the
172 MFI of secondary antibody-conjugated to PE, or FcR protein-conjugated to PE for each

173 bead region was measured on the Luminex Intelliflex to quantify antigen-specific
174 immunoglobulin isotypes and FcR responses in each sample at 0- and 28-days post
175 vaccination [30].

176 ***Antibody-dependent complement deposition (ADCD)***

177 Serum (1:15 dilution) was added to the MagPlex antigen coated beads. Plates were
178 incubated, placed on a magnet, and washed 3 times with 1% BSA. Lyophilized Low-Tox
179 Guinea Pig Complement (Cedarlane) was reconstituted in ice-cold dH2O and diluted 1:25
180 in Gelatin Veronal buffer with Mg^{2+} & Ca^{2+} (GVB++) (Boston Bio). Diluted complement
181 protein was added to each well followed by incubation at 37C. IgG goat anti-guinea pig C3
182 (MP Biomedicals) was diluted 1:500 in 0.1% BSA and added to each well. After incubation,
183 Donkey-anti goat IgG secondary antibody-PE (ThermoFisher) was diluted 1:200 in 0.1% BSA
184 and added to each well. Beads were resuspended in 0.1% BSA and run on the Luminex
185 Intelliflex.

186 ***Antibody-dependent NK cell cytotoxicity (ADNK)***

187 Natural killer (NK) cells were isolated from donor blood. Whole blood was spun
188 down with a Ficoll gradient to harvest PBMCs and NK cells isolated from PBMCs using the
189 MagniSort™ Human NK cell Enrichment Kit (ThermoFisher) with adjustment to a final
190 concentration of 1.5 x 10^6 cells/mL in R10 media, and IL-15 (1ng/mL, Abcam) was added
191 and incubated overnight. Plates were coated with 3mg/mL antigen (ancestral, BA.5,
192 XBB.1.5, and JN.1 spike proteins – SeroNet), blocked with 5% BSA, washed, and dried
193 before adding serum (1:100 dilution). Inhibitor cocktail (2.5 uL CD107a-PeCy5 (BD
194 Bioscience - BDB555802) + 0.5mL BFA (Millipore Sigma) + 1 uL Golgi Stop (BD Bioscience)

195 + 9mL R10 media) was added to each well, incubated, and surface staining cocktail (1uL
196 CD3-Pacific Blue (BD Bioscience - BDB558117) + 1mL CD56-PE-Cy7 (BD Bioscience -
197 BDB557747) + 1mL CD16-APC-Cy7 (BD Bioscience - BDB557758) + 7mL PBS) is added to a
198 V-bottom 96 well plate. NK cells were transferred to the V-bottom 96 well plate with pre-
199 added surface stain cocktail and incubated. Cells are spun down, supernatant removed,
200 and Perm A (ThermoFisher) was added to each well. Cells were washed and Intracellular
201 staining cocktail (1mL IFNγ-APC (BD Bioscience -) + 1mL MIP1-B-PE (BD Bioscience -
202 BDB550078) + 48mL Perm B (ThermoFisher) was added to each well. Plates were washed,
203 cells were resuspended in PBS and run on a Symphony A3 through the Bloomberg Flow
204 Cytometry and Immunology Core. Gating strategy as follows: NK cells- CD3-, CD16+,
205 CD56+ with reported cell populations including IFNγ+, CD107a+ and MIP1-B+ NK cells.

206 ***Antibody-dependent neutrophil phagocytosis (ADNP)***

207 Antigens (ancestral, BA.5, XBB.1.5, and JN.1 spike proteins – SeroNet) were
208 biotinylated with the BirA biotin-ligation kit (Avidity) and coupled to FluoSpheres™
209 NeutrAvidin™-Labeled Microspheres, 1.0 µm, yellow-green fluorescent (505/515)
210 (ThermoFisher). Antigen was combined with Neutravidin beads and incubated. Serum was
211 diluted 1:100 in PBS and incubated with antigen coated beads. During incubation, cells
212 were isolated from donor blood. Whole blood was collected into CPT tubes and spun at
213 1000rpm for 30min. Granulocytes were collected from below the density gradient. Cells
214 were suspended 1:10 in ACK Lysis buffer and incubated at RT for 5 min to lyse red blood
215 cells. Cells were washed and resuspended in 10mL of PBS. Plates were washed with PBS,
216 200mL of neutrophil solution (5 x 10^6 cells/plate) was added to each well, incubated,

217 spun at 500g for 5 min, and cells were resuspended in extracellular staining solution (0.5
218 mL APC CD66b (BioLegend - 305117) + 19.5mL PBS / well) and incubated for 15min
219 covered with foil at RT. After staining, plates were washed and resuspended in 4% PFA to fix
220 cells, washed and resuspended in PBS. Plates were run on the Attune NxT flow cytometer.
221 Gating on CD66b+ cells (neutrophils) followed by bead+ neutrophils, stained with APC.
222 Data are reported as a PhagoScore, calculated as (% bead positive neutrophils) *
223 (geometric MFI of each cell) [31].

224 ***Antibody-dependent cellular phagocytosis (ADCP)***

225 THP-1 cells, a human monocytic cell line, were plated 2.5 x 10^4 per well. Cells were
226 grown in suspension and diluted with warm R10 media. Following immune complex
227 formation, assay plates are washed with PBS and centrifuged at 2000g for 10min. The THP-
228 1 cells were added, and plates were incubated O/N at 37C. THP-1 cells were fixed, washed,
229 and resuspended in PBS. Plates are run on the Attune NxT flow cytometer. Gating included
230 bead+ single-cells stained with APC, representing THP-1 cells that have phagocytosed
231 bead. Data are reported as a PhagoScore, calculated as (% bead positive neutrophils) *
232 (geometric MFI of each cell) [32].

233 ***Ex vivo flow cytometry staining***

234 PBMCs were used to assess phenotype and function of immune cells. For broad
235 immune cell phenotyping (BIP), cells were stained for viability with Biolegend Live/Dead
236 Zombie NIR Fixable Viability Dye (423105) and BD Biosciences Fc Block™ (564219). Cell
237 surface staining was performed with surface antibody cocktail mix (**Supplementary**
238 **Methods Table 1A**). Cells were fixed and permeabilized with a 1X Fixation/Permeabilization

239 buffer from eBioscience FoxP3/Transcription Factor Staining Buffer Set. Intracellular
240 staining was performed with intracellular antibody cocktail mix (**Supplementary Methods**
241 **Table 1B**). Cells were resuspended in 1% paraformaldehyde and run on the 4-laser (16UV-
242 16V-15B-8R) Cytek Biosciences Aurora spectral flow cytometer. Data were exported for
243 further analysis in FlowJo for analysis (**Supplemental Figure 4**).

244 Intracellular cytokine flow cytometry staining was used to assess antigen-specific
245 cytokine production and T cell phenotypic and functional profiles. Cryopreserved PBMCs
246 were thawed, rested, and cultured overnight with 1 mg/mL peptide pools consisting of 315
247 peptides (15mers with 11 amino acid overlap) spanning the ancestral SARS-CoV-2 spike
248 protein (JPT Peptide Technologies, PM-WCPV-S-1) or a DMSO (unstimulated) control. After
249 overnight incubation, cells were washed and stained for flow cytometry as described for
250 BIP with the following variation: staining for viability was with Invitrogen Live/Dead Fixable
251 Blue Dead Cell Stain (L34962) and with T-cell panel surface and intracellular cytokine
252 antibody cocktails (**Supplementary Methods Table 2A-B**). For ICS, data were processed
253 using biexponential transformation and exported for further analysis in FlowJo to assess
254 cytokine-producing, antigen-specific T cells (**Supplemental Figure 5**). Polyfunctionality of
255 these T cells was analyzed with Pestle v2.0 and SPICE 6 v6.1.

256 ***Statistical analyses***

257 GraphPad Prism v10.1 was used to perform univariate analyses with details about
258 statistical tests used for each dataset in figure legends. Spearman correlations of systems
259 serology measures were visualized in heatmaps generated using R v4.2.3 and version
260 1.0.12 of the package "pheatmap" (https://cran.r-project.org/web/packages/pheatmap

261 [33]. For ADNP and ADNK assays, data were averaged across two healthy donors. Flow FCS
262 files were analyzed using FlowJo v10 (10.8.1) software. Gating strategy for BIP and ICS can
263 be found in **Supplementary Figures 1** and **2**, respectively. ICS and BIP data were exported
264 from Pestle v2.0 and SPICE 6 v6.1 for further statistical analyses detailed in figure legends.
265

266 **Results**

267 ***Pregnancy alters IgG subtype dominance in response to novel variants***

268 Because SARS-CoV-2 nucleocapsid (N) antibodies are not generated by mRNA
269 vaccines targeted to S protein, this can be used as a proxy for SARS-CoV-2 infection [34],
270 with recognized limitations [25]. There was no increase in either anti-N IgG **(Figure 1A)** or in
271 any subclass of IgG **(Supplemental Figure 1A)** in any participants, suggesting that no one
272 was infected with SARS-CoV-2 during their study enrollment window. However, all
273 participants had detectable anti-N IgG levels highlighting prior exposure to SARS-CoV-2 in
274 our cohort. Luminex bead assays were used to comprehensively characterize the antibody
275 response generated by vaccination against SARS-CoV-2 vaccine antigens (ancestral and
276 BA.5 S) and other variants (XBB.1.5 and JN.1 S). COVID-19 boosters induced IgG in both
277 pregnant and non-pregnant females to vaccine and circulating variants **(Figure 1B)**. Prior to
278 vaccination, total IgG to ancestral S and BA.5 S was high in both cohorts as SARS-CoV-2
279 exposure through infection and prior vaccination is pervasive in the general population
280 [35]. However, there were distinct differences in the IgG subtype dominating this response.
281 There was IgG1 subtype dominance among non-pregnant, but not pregnant, females
282 **(Figure 1C-F).** While contributing to a small proportion of total IgG generated in response

283 to vaccination, pregnant women were more likely to induce anti-S IgG3 than non-pregnant
284 females **(Supplemental Figure 1 B-E).**

285 ***Pregnancy reduces the cross-neutralizing capacity of antibodies recognizing SARS-***
286 ***CoV-2 variants***

287 The ratio of IgG1:IgG3 has been shown to be predictive of SARS-CoV-2 neutralization
288 capacity [36]. Compared to non-pregnant females, pregnant women had reduced
289 IgG1:IgG3 ratios, particularly to circulating variants, demonstrating that the dominant IgG1
290 response in non-pregnant females may be indicative of broader cross-neutralization
291 **(Figure 2A-D).** This was reflected by reduced live virus neutralizing antibody [25] titers in
292 pregnant compared with non-pregnant women to variants. Both cohorts showed a rise in
293 neutralizing antibody titers to ancestral and BA.5 viruses after vaccination and were able to
294 effectively neutralize these viruses **(Figure 2E-F)**. Pregnant women, however, had
295 significantly lower nAb titers than non-pregnant females, with many pregnant women
296 failing to reach the limit of detection **(Figure 2G-H)**. In response to XBB.1.5, while
297 vaccination significantly increased nAb titers in both groups, these responses were
298 significantly higher in non-pregnant than pregnant females. Likewise, among non-pregnant
299 females, vaccination boosted nAb titers against JN.1; there was, however, no vaccine-
300 induced increase in nAb titers among pregnant women, with only 2/7 surpassing the limit of
301 detection. **(Figure 2G-H)**. These data suggest that there is reduced breadth and cross-
302 reactivity to variants after COVID-19 boosting among pregnant compared with non-
303 pregnant females.

304 ***Fc receptor affinity is not maintained in pregnant women against novel variants***

305 While neutralizing antibody titers are considered a correlate of protection for SARS-
306 CoV-2 infection [37], non-neutralizing functions also are important and may contribute to
307 robust protection from severe disease [38]. Data from mouse models suggest FcR binding
308 affinity and its associated effector functions are necessary for preventing severe COVID-19
309 disease [39]. To further understand protection provided by mRNA boosters in pregnant
310 women, we investigated FcR binding affinity. Antibody Fc binding affinity to FcγRIIA-R,
311 FcγRIIA-H, FcγRIIb, FcγRIIIA-V, FcγRIIIA-F, FcγRIIIB, FcRn, and FcαR was assessed by a
312 multiplexed Luminex bead assay. FcR binding affinity was similarly induced by vaccination
313 in response to ancestral and BA.5 vaccine antigens among both non-pregnant and
314 pregnant females **(Figure 3A-B).** While non-pregnant females saw similar increases in FcR
315 affinity to non-vaccine antigens following vaccination, vaccination did not induce changes
316 in FcR affinity in pregnant women, with no increase in affinity to 4/6 FcγRs in response to
317 XBB1.5 and 2/6 FcγRs in response to JN.1 (**Figure 3C-D**).

318 ***Non-neutralizing antibody functions and nAb are negatively correlated among***
319 ***pregnant women***

320 In order to understand how Fc binding affinity contributes to immunity generated by
321 COVID-19 vaccination, several non-neutralizing antibody functions were assessed. Non-
322 neutralizing functions aid in the clearance of infected cells through recruiting effector cells
323 [40]. Antibody dependent complement deposition (ADCD) was analyzed with a multiplexed
324 Luminex bead assay to measure antibody binding to complement protein C3 as a broad
325 indicator of the ability of serum antibody to induce activation of the complement cascade
326 [30]. ADCD was induced by vaccination in both cohorts in response to only XBB.1.5.

327 (**Figure 4A**). As ADCD to ancestral and BA.5 S was high in pre-vaccination samples, it is
328 likely that there were high preexisting immune responses through complement activation in
329 both cohorts.

330 In pregnancy, macrophage inflammatory protein (MIP)-1β+ NK cells are found at the
331 maternal-fetal interface and are important for successful implantation and placentation
332 [41]. In NK cells, MIP-1β acts as a chemoattractant in response to activation [42]. Antibody-
333 dependent NK cell cytotoxicity (ADNK) can be measured through MIP-1β production by NK
334 cells [43]. MIP-1β+ NK cells were uniquely elevated in pregnant women following
335 vaccination when compared to non-pregnant females (**Figure 4B**). In NK cells, interferon
336 gamma (IFNγ) acts as an antiviral cytokine to promote further accumulation, activation,
337 and cytotoxicity of NK cells [44]. As an additional readout of ADNK, NK cell IFNγ production
338 post-vaccination was elevated in pregnant women in response to BA.5 S, and in non-
339 pregnant females in response to JN.1 S **(Supplemental Figure 2A).** There were no changes
340 post-vaccination in NK cell degranulation, as marked by CD107a+ NK cells, among either
341 cohort **(Supplemental Figure 2B)**.

342 Antibody-dependent cellular phagocytosis (ADCP) and antibody-dependent
343 neutrophil phagocytosis (ADNP) assess the ability of antibody to induce macrophage and
344 neutrophil phagocytosis of antigen, respectively, and are reported as a PhagoScore [31],
345 representing both the function and number of beads phagocytosed. ADCP and ADNP
346 decreased following vaccination against vaccine and variant antigens (**Figure 4C-D**). This is
347 likely indicative of a shift towards neutralization and away from non-neutralizing cellular
348 functions, a phenomenon that has been documented in the context of repeat vaccination

349 and may be a result of immune imprinting mechanisms [45]. Correlation analyses revealed
350 significant negative correlations between nAb titers and ADNP PhagoScores among
351 pregnant women only, further suggesting a shift away from neutralization, and towards
352 non-neutralizing neutrophil phagocytosis among pregnant women (**Figure 4E-H**). In non-
353 pregnant females, correlations were not significant, suggesting antibody responses marked
354 by both cellular non-neutralizing and neutralizing antibody function, indicative of a more
355 comprehensive and multi-pronged immune response generated by vaccination.

356 ***Altered correlations among IgG subclasses and antibody functional phenotypes in***
357 ***pregnant women***

358 Correlation matrices can be used to examine complex relationships between
359 antibody isotypes and effector functions assessed by systems serology [46]. These
360 analyses can highlight isotype dependence and may reveal differences in subclass
361 functionality [46]. Spearman correlation matrices were generated to assess correlations
362 between Ig isotypes and FcR affinity and antibody functional properties post-vaccination in
363 response to vaccine and variant viruses (**Figure 5**). Matrices were most different between
364 pregnant and non-pregnant women for variants, with fewer strong correlations in pregnant
365 than non-pregnant women. Among non-pregnant women, IgG1 was positively and IgG3
366 was negatively correlated with FcR binding as well as neutralizing and non-neutralizing
367 antibody functions, particularly against variants. This trend was reversed in pregnant
368 women, with positive trends with IgG3 and negative trends with IgG1. These data further
369 implicate the reduced IgG1:IgG3 ratio and isotype subclass switching as functionally
370 altering antibody-mediated immunity in pregnant women.

371 ***Decreased polyfunctional CD4⁺ T cells responses in pregnant women***

372 Because immunoglobulin subtype switching depends on CD4⁺ T cell help and
373 cytokine production [47], we hypothesized that differences in CD4⁺ T cell cytokine
374 production between pregnant and nonpregnant females might contribute to differences in
375 isotype switching and IgG subtypes. We assessed intracellular cytokine production by
376 CD4+ T cells in pregnant and non-pregnant women in response to ancestral S peptide
377 pools [48, 49]. Intracellular cytokine staining of CD4+ T cells in response to ancestral S
378 peptide stimulation at post-vaccination timepoints demonstrated IFNγ+ monofunctional
379 dominance in pregnant women, represented by an expansion of the dark purple slice
380 (**Figure 6A**). In CD4+ T cells, IFNγ production is known to modulate class switching in B
381 cells, particularly favoring IgG3 over IgG1 [50-52]. Conversely, non-pregnant female
382 participants demonstrated more broadly polyfunctional CD4+ T cell responses, defined as
383 producing two or more cytokines and highlighted by the arcs (**Figure 6B**). A greater
384 proportion of polyfunctional CD4+ T cells in the non-pregnant females were IL-21+,
385 represented by the green arc (**Figure 6B**). IL-21 is a cytokine that induces B cells to
386 differentiate into antibody secreting cells [53] and has been linked to improved antibody
387 responses to vaccination [48, 54-56]. Polyfunctional CD4+ T cell responses can enhance
388 nAb titers and immunity following vaccination against multiple pathogens, including SARS-
389 CoV-2 [57-59].

390 ***Polymorphonuclear myeloid-derived suppressor cells are increased during pregnancy***

391 Polymorphonuclear myeloid-derived suppressor cells (PMN-MDSCs) have
392 previously been studied in the context of pregnancy, as they are required to maintain

393 maternal-fetal tolerance and are critical for fetal development [60, 61]. Their role, however,
394 has not been defined in the context of vaccination during pregnancy. There were no
395 detectable PMN-MDSCs in nonpregnant women, whereas the percentage in pregnant
396 women ranged from 0 to 1.5% of live PBMCs (**Supplemental Figure 3A**). The percentage of
397 low-density neutrophils also tended to be greater in pregnant women (**Supplemental**
398 **Figure 3B**), but small sample sizes preclude deeper analysis. The percentages of both
399 PMN-MDSCs and neutrophils were negatively correlated with CD4+ T cell cytokine
400 production in pregnant women (**Supplemental Figure 3C**).
401

402 **Discussion**

403 Through broad characterization of the antibody landscape following COVID-19
404 vaccination, pregnancy was associated with reduced cross-protective antibody responses,
405 reflected in decreased IgG1:IgG3 ratios, nAb titers, and FcR binding affinity in pregnant
406 compared with non-pregnant women. Previous studies have assessed the antibody profile
407 generated by COVID-19 vaccination during pregnancy [18, 21, 62], with a focus on
408 transplacental antibody transfer and protection of babies and infants from severe disease.
409 One study showed limited cross-recognition in pregnant women to non-vaccine antigens
410 after the first doses of ancestral vaccines, with no comparisons to non-pregnant controls
411 [18]. Our data illustrate that pregnancy is associated with reduced isotype class switching
412 and nAb responses to variants as compared with non-pregnant controls. Continuing efforts
413 to assess antibody responses to updated vaccines remains critical to understanding cross-
414 protection to variants in circulation.

415 SARS-CoV-2 has continued to rapidly evolve and mutate into new variants to escape
416 adaptive immune responses [63]. In 2022, Omicron variants became dominant in
417 circulation, largely due to an ability to evade nAb generated by ancestral vaccines and
418 natural infections [64]. New variants with the ability to evade nAb continue to emerge and
419 dominate, with XBB.1.5. appearing in October 2022 and peaking in January of 2023, after
420 the inclusion of BA.5 in bivalent booster vaccines was established [65]. By the time XBB.1.5
421 monovalent boosters were accessible, a new variant, JN.1 caused 60% of global cases [65,
422 66]. This reflects a limitation of annual vaccine campaigns in which there is a mismatch
423 between dominate circulating strains and updated booster vaccines because variants
424 continue to emerge between annual vaccines strain updates. While mRNA technology has
425 increased the speed in which companies can adapt updated vaccines to emerging
426 variants, development of a new booster vaccine still takes several months [67]. Thus,
427 government officials and researchers must work collaboratively to select strains for
428 booster vaccines that will elicit the greatest breadth of immunity [67]. In our study, almost
429 all women were vaccinated against ancestral and BA.5 (bivalent boosters), while XBB.1.5.
430 was the dominant variant in circulation. Our data provide mechanistic evidence that
431 pregnant women have limited cross-protective antibodies that could be critical to protect
432 pregnant women and their babies from severe disease caused by emerging variant.
433 With repeated exposure to antigen through natural infection and booster vaccines,
434 antibody responses to COVID-19 vaccines have evolved and correlates of protection have
435 changed. Total IgG and nAb titers are considered adequate correlates of protection against
436 COVID-19, similar to other acute respiratory infectious diseases [68]. Recent data have

437 suggested that to mount sufficient protection, antibodies against SARS-CoV-2 must
438 possess both neutralizing and non-neutralizing functions as correlates of protection [69].
439 As nAb titers wane and symptomatic cases rise, hospitalization rates among the general
440 population remain low [70]. This provides evidence that other antibody characteristics may
441 be important for protection from severe disease. Our data demonstrate that pregnant
442 women have reduced FcR binding and nAb responses combined with elevated ADNK and
443 ADNP, especially to non-vaccine antigens. These data might suggest that the shift from
444 neutralizing to non-neutralizing antibody responses against emerging variants could reduce
445 protection in pregnant women.

446 Our data suggest that reduced class switching and T cell polyfunctionality may
447 contribute to limited cross-reactivity of antibodies during pregnancy. There is trend for
448 PMN-MDSCs in PBMCs to be more frequent among pregnant than non-pregnant, which
449 might contribute to suppressed CD4+ T cell cytokine production and proliferation [36].
450 CD4+ T cells are critical for generation of high affinity, class switched antibodies and
451 contribute to vaccine-induced protection against COVID-19 [71]. Our data suggest that
452 reduced T-cell polyfunctionality during pregnancy may limit protection conferred to novel
453 variants. IL-21+ CD4+ T cells are correlated with enhanced vaccine responses, including
454 COVID-19 vaccine responses [55]. Pregnant women showed reduced expansion of IL-21+
455 CD4+ T-cells, potentially contributing to reduced Ig class switching and the generation of
456 nAb responses in pregnant women [48, 54-56]. Additionally, expansion of IFNγ+
457 monofunctional CD4+ T cells may further contribute to reduced IgG1:IgG3 ratios among
458 pregnant women as these cells promote IgG3 bias in B cells [50-52].

The small sample size is a limitation of this study and was associated with challenges recruiting pregnant women. Previous studies have shown the impact of trimester on immune responses generated by COVID-19 vaccination [12, 72]. In the present study, sample size limited our ability to assess trimester differences, with 6/7 pregnant females enrolled in our study being vaccinated in the second trimester of pregnancy. While 232 pregnant women were approached during the study enrollment window, only 7 completed the study. This likely reflects the limited COVID-19 vaccine uptake among pregnant women, which we show is caused by numerous factors across the care continuum that contribute to COVID-19 vaccine hesitancy in this population (Parish et al. 2025b, submitted). Identification of points of public health intervention to effectively increase vaccine uptake among pregnant women is needed.

There are many factors contributing to COVID-19 vaccine hesitancy; lack of confidence in vaccine safety, however, is a large contributor [13], especially with pregnant women being excluded from early COVID-19 vaccine trials [73]. Continued research and public health efforts to disseminate information on the safety and necessity of updated COVID-19 vaccination during pregnancy are needed to address gaps in understanding and to increase vaccine uptake.

Acknowledgements. We thank the clinical coordinators and vaccinees for making this study possible. We are especially grateful to Kimberly Jones-Beatty and Michelle Ufua for their assistance with recruitment. Thank you to Galit Alter, Ryan McNamara, and Taras Chicz for graciously training lab members and sharing protocols to develop systems

serology methods. We thank Prakash Srinivasan for the use of the Attune Nxt flow cytometer.

Funding. FDA CERSI U01FD005942 (SLK), NIH NIAID 75N93021C00045 (AP, RR), NIH NCI U54 CA260492 (SLK, ALC).

Data Availability

All anonymized data that support the findings of this study and source data for the figures are available through the NIH/NCI Serological Sciences Network for COVID-19 (SeroNet) data repository, accessible via ImmPort (https://www.immport.org) under study accession XXXXXXX. All other data are available from the corresponding author upon reasonable request.

Author Contributions

SLK, IB, AP, and ALC conceptualized the experimental design and group comparisons for this study. MAP, H-SP, JSL, LStC, PS, IB, JS, KF, RR, and ALC identified, acquired, stored, and distributed patient samples and clinical and demographic data for analyses. MAP, H-SP, PC, AW and JSL developed and validated serological assays. MAP, JS, LG and H-SP processed samples and completed technical assays. MAP, KR, and AY conducted statistical analyses. MAP, LG, KR, ALC, and SLK developed all tables and figures. MAP, ALC, SLK wrote the initial draft of the manuscript. All authors provided substantive edits and approved the final draft of the manuscript.

503

504 **References**

505

506 1. Engjom, H.M., et al., *Perinatal outcomes after admission with COVID-19 in*
507 *pregnancy: a UK national cohort study.* Nature Communications, 2024. **15**(1): p.
508 3234.
509 2. Brioschi Dos Santos, A.P., et al., *The impact of COVID-19 on maternal death and*
510 *fetal death, a cohort study in Brazil.* PLoS One, 2023. **18**(8): p. e0290343.
511 3. St Clair, L.A., et al., *Reduced control of SARS-CoV-2 infection associates with lower*
512 *mucosal antibody responses in pregnancy.* mSphere, 2024. **9**(3): p. e0081223.
513 4. Strid, P., et al., *Coronavirus Disease 2019 (COVID-19) Severity Among Women of*
514 *Reproductive Age With Symptomatic Laboratory-Confirmed Severe Acute*
515 *Respiratory Syndrome Coronavirus 2 (SARS-CoV-2) Infection by Pregnancy Status-*
516 *United States, 1 January 2020-25 December 2021*. Clin Infect Dis, 2022. **75**(Suppl 2):
517 p. S317-s325.
518 5. Wei, S.Q., et al., *The impact of COVID-19 on pregnancy outcomes: a systematic*
519 *review and meta-analysis.* Cmaj, 2021. **193**(16): p. E540-e548.
520 6. Sessa, R., et al., *SARS-CoV-2 Infection in Pregnancy: Clues and Proof of Adverse*
521 *Outcomes*. Int J Environ Res Public Health, 2023. **20**(3).
522 7. Creisher, P.S., et al., *Adverse outcomes in SARS-CoV-2-infected pregnant mice are*
523 *gestational age-dependent and resolve with antiviral treatment*. J Clin Invest, 2023.
524 **133**(20).
525 8. Ciapponi, A., et al., *Safety of COVID-19 vaccines during pregnancy: A systematic*
526 *review and meta-analysis*. Vaccine, 2023. **41**(25): p. 3688-3700.
527 9. Razzaghi, H., et al., *COVID-19 vaccination coverage and intent among women aged*
528 *18-49 years by pregnancy status, United States, April-November 2021*. Vaccine,
529 2022. **40**(32): p. 4554-4563.
530 10. Katherine E. Kahn, E.G., Hilda Razzaghi, Tara C. Jatlaoui, Tami H. Skoff, Sascha R.
531 Ellington, Carla L. Black, *Flu, Tdap, and COVID-19 Vaccination Coverage Among*
532 *Pregnant Women – United States, April 2024*. 2024.
533 11. Razzaghi H, K.K., Calhoun K, et al., *Influenza, Tdap, and COVID-19 Vaccination*
534 *Coverage and Hesitancy Among Pregnant Women — United States, April 2023*.
535 MMWR Morb Mortal Wkly Rep, 2023.
536 12. Norman, M., et al., *Neonatal Outcomes After COVID-19 Vaccination in Pregnancy.*
537 Jama, 2024. **331**(5): p. 396-407.
538 13. Casubhoy, I., et al., *A scoping review of global COVID-19 vaccine hesitancy among*
539 *pregnant persons*. npj Vaccines, 2024. **9**(1): p. 131.
540 14. Oliver, J., et al., *Drivers of COVID-19 vaccine hesitancy among women of*
541 *childbearing age in Victoria, Australia: A descriptive qualitative study.* Vaccine: X,
542 2022. **12**: p. 100240.
543 15. Hsu, A.L., et al., *Sources of Vaccine Hesitancy: Pregnancy, Infertility, Minority*
544 *Concerns, and General Skepticism*. Open Forum Infectious Diseases, 2021. **9**(3).

545 16. Chavan, M., et al., *COVID-19 Vaccination in Pregnancy: The Benefits Outweigh the*
546 *Risks*. J Obstet Gynaecol Can, 2021. **43**(7): p. 814-816.
547 17. Kay, A.W. and C.A. Blish, *Immunogenicity and Clinical Efficacy of Influenza*
548 *Vaccination in Pregnancy*. Front Immunol, 2015. **6**: p. 289.
549 18. Lopez, P.A., et al., *Placental transfer dynamics and durability of maternal COVID-19*
550 *vaccine-induced antibodies in infants*. iScience, 2024. **27**(3): p. 109273.
551 19. Munoz, F.M., et al., *COVID-19 booster vaccination during pregnancy enhances*
552 *maternal binding and neutralizing antibody responses and transplacental antibody*
553 *transfer to the newborn*. Vaccine, 2023. **41**(36): p. 5296-5303.
554 20. Cassidy, A.G., et al., *Assessment of Adverse Reactions, Antibody Patterns, and 12-*
555 *month Outcomes in the Mother-Infant Dyad After COVID-19 mRNA Vaccination in*
556 *Pregnancy*. JAMA Netw Open, 2023. **6**(7): p. e2323405.
557 21. Atyeo, C., et al., *COVID-19 mRNA vaccines drive differential antibody Fc-functional*
558 *profiles in pregnant, lactating, and nonpregnant women*. Sci Transl Med, 2021.
559 **13**(617): p. eabi8631.
560 22. Ackerman, M.E., D.H. Barouch, and G. Alter, *Systems serology for evaluation of HIV*
561 *vaccine trials*. Immunol Rev, 2017. **275**(1): p. 262-270.
562 23. Fall, A., et al., *The displacement of the SARS-CoV-2 variant Delta with Omicron: An*
563 *investigation of hospital admissions and upper respiratory viral loads*. EBioMedicine,
564 2022. **79**: p. 104008.
565 24. Dhakal, S., et al., *Sex Differences in Lung Imaging and SARS-CoV-2 Antibody*
566 *Responses in a COVID-19 Golden Syrian Hamster Model*. mBio, 2021. **12**(4): p.
567 e0097421.
568 25. Dhakal, S., et al., *Reconsideration of Antinucleocapsid IgG Antibody as a Marker of*
569 *SARS-CoV-2 Infection Postvaccination for Mild COVID-19 Patients*. Open Forum
570 Infect Dis, 2023. **10**(1): p. ofac677.
571 26. Lee, J.M., et al., *Three doses of COVID-19 mRNA vaccine induce class-switched*
572 *antibody responses in inflammatory arthritis patients on immunomodulatory*
573 *therapies*. Front Immunol, 2023. **14**: p. 1266370.
574 27. Li, M., et al., *Convalescent plasma with a high level of virus-specific antibody*
575 *effectively neutralizes SARS-CoV-2 variants of concern*. Blood Adv, 2022. **6**(12): p.
576 3678-3683.
577 28. Klein, S.L., et al., *Sex, age, and hospitalization drive antibody responses in a COVID-*
578 *19 convalescent plasma donor population*. J Clin Invest, 2020. **130**(11): p. 6141-
579 6150.
580 29. Karger, A.B., et al., *The Serological Sciences Network (SeroNet) for COVID-19: Depth*
581 *and Breadth of Serology Assays and Plans for Assay Harmonization*. mSphere, 2022.
582 **7**(4): p. e0019322.
583 30. Chung, A.W., et al., *Dissecting Polyclonal Vaccine-Induced Humoral Immunity*
584 *against HIV Using Systems Serology*. Cell, 2015. **163**(4): p. 988-98.
585 31. Karsten, C.B., et al., *A versatile high-throughput assay to characterize antibody-*
586 *mediated neutrophil phagocytosis*. J Immunol Methods, 2019. **471**: p. 46-56.

587 32. Loos, C., et al., *Systems serology-based comparison of antibody effector functions*
588 *induced by adjuvanted vaccines to guide vaccine design*. npj Vaccines, 2023. **8**(1): p.
589 34.
590 33. Kolde, R., *Pretty Heatmaps*. 2018. p. Implementation of heatmaps that offers more
591 control over dimensions and appearance.
592 34. Gaeta, A., et al., *Anti-N SARS-CoV-2 assays for evaluation of natural viral infection*. J
593 Immunol Methods, 2023. **518**: p. 113486.
594 35. Swadźba, J., et al., *High Concentration of Anti-SARS-CoV-2 Antibodies 2 Years after*
595 *COVID-19 Vaccination Stems Not Only from Boosters but Also from Widespread,*
596 *Often Unrecognized, Contact with the Virus*. Vaccines (Basel), 2024. **12**(5).
597 36. Chen, W., et al., *The kinetics of IgG subclasses and contributions to neutralizing*
598 *activity against SARS-CoV-2 wild-type strain and variants in healthy adults*
599 *immunized with inactivated vaccine*. Immunology, 2022. **167**(2): p. 221-232.
600 37. Sun, K., et al., *SARS-CoV-2 correlates of protection from infection against variants of*
601 *concern*. Nature Medicine, 2024. **30**(10): p. 2805-2812.
602 38. Izadi, A. and P. Nordenfelt, *Protective non-neutralizing SARS-CoV-2 monoclonal*
603 *antibodies*. Trends Immunol, 2024. **45**(8): p. 609-624.
604 39. Mackin, S.R., et al., *Fc-γR-dependent antibody effector functions are required for*
605 *vaccine-mediated protection against antigen-shifted variants of SARS-CoV-2*. Nat
606 Microbiol, 2023. **8**(4): p. 569-580.
607 40. Chandler, T.L., et al., *Protective mechanisms of nonneutralizing antiviral antibodies*.
608 PLoS Pathog, 2023. **19**(10): p. e1011670.
609 41. Du, M.R., S.C. Wang, and D.J. Li, *The integrative roles of chemokines at the*
610 *maternal-fetal interface in early pregnancy*. Cell Mol Immunol, 2014. **11**(5): p. 438-
611 48.
612 42. Bluman, E.M., et al., *Human natural killer cells produce abundant macrophage*
613 *inflammatory protein-1 alpha in response to monocyte-derived cytokines*. J Clin
614 Invest, 1996. **97**(12): p. 2722-7.
615 43. Boudreau, C.M., et al., *Antibody-mediated NK cell activation as a correlate of*
616 *immunity against influenza infection*. Nature Communications, 2023. **14**(1): p. 5170.
617 44. Lin, Q., et al., *IFN-γ-dependent NK cell activation is essential to metastasis*
618 *suppression by engineered Salmonella*. Nature Communications, 2021. **12**(1): p.
619 2537.
620 45. Tortorici, M.A., et al., *Persistent immune imprinting occurs after vaccination with the*
621 *COVID-19 XBB.1.5 mRNA booster in humans*. Immunity, 2024. **57**(4): p. 904-911.e4.
622 46. Atyeo, C., et al., *Distinct Early Serological Signatures Track with SARS-CoV-2*
623 *Survival*. Immunity, 2020. **53**(3): p. 524-532.e4.
624 47. Sha, Z. and R.W. Compans, *Induction of CD4(+) T-cell-independent immunoglobulin*
625 *responses by inactivated influenza virus*. J Virol, 2000. **74**(11): p. 4999-5005.
626 48. Thompson, E.A., et al., *Heterologous versus homologous boosting elicits*
627 *qualitatively distinct, BA.5-cross-reactive T cells in transplant recipients*. JCI Insight,
628 2023. **8**(10).

49. Roznik, K., et al., *COVID-19 vaccination induces distinct T-cell responses in pediatric solid organ transplant recipients and immunocompetent children*. NPJ Vaccines, 2024. **9**(1): p. 73.
50. Peng, S.L., S.J. Szabo, and L.H. Glimcher, *T-bet regulates IgG class switching and pathogenic autoantibody production*. Proc Natl Acad Sci U S A, 2002. **99**(8): p. 5545-50.
51. Alspach, E., D.M. Lussier, and R.D. Schreiber, *Interferon γ and Its Important Roles in Promoting and Inhibiting Spontaneous and Therapeutic Cancer Immunity*. Cold Spring Harb Perspect Biol, 2019. **11**(3).
52. Mohr, E., et al., *IFN-{gamma} produced by CD8 T cells induces T-bet-dependent and -independent class switching in B cells in responses to alum-precipitated protein vaccine*. Proc Natl Acad Sci U S A, 2010. **107**(40): p. 17292-7.
53. Wang, S., et al., *IL-21 drives expansion and plasma cell differentiation of autoreactive CD11chiT-bet+ B cells in SLE*. Nature Communications, 2018. **9**(1): p. 1758.
54. Pallikkuth, S., et al., *Upregulation of IL-21 receptor on B cells and IL-21 secretion distinguishes novel 2009 H1N1 vaccine responders from nonresponders among HIV-infected persons on combination antiretroviral therapy*. J Immunol, 2011. **186**(11): p. 6173-81.
55. Malahe, S.R.K., et al., *The role of interleukin-21 in COVID-19 vaccine-induced B cell-mediated immune responses in patients with kidney disease and kidney transplant recipients*. Am J Transplant, 2023. **23**(9): p. 1411-1424.
56. Fan, W., Y. Wan, and Q. Li, *Interleukin-21 enhances the antibody avidity elicited by DNA prime and MVA boost vaccine*. Cytokine, 2020. **125**: p. 154814.
57. Darrah, P.A., et al., *Multifunctional TH1 cells define a correlate of vaccine-mediated protection against Leishmania major*. Nat Med, 2007. **13**(7): p. 843-50.
58. Rakshit, S., et al., *Polyfunctional CD4 T-cells correlating with neutralising antibody is a hallmark of COVISHIELDTM and COVAXIN® induced immunity in COVID-19 exposed Indians*. npj Vaccines, 2023. **8**(1): p. 134.
59. Li, L., et al., *In-depth analysis of SARS-CoV-2-specific T cells reveals diverse differentiation hierarchies in vaccinated individuals*. JCI Insight, 2022. **7**(7).
60. Shi, M., et al., *Continuous activation of polymorphonuclear myeloid-derived suppressor cells during pregnancy is critical for fetal development*. Cellular & Molecular Immunology, 2021. **18**(7): p. 1692-1707.
61. Li, C., et al., *Upregulated TRAIL and Reduced DcR2 Mediate Apoptosis of Decidual PMN-MDSC in Unexplained Recurrent Pregnancy Loss*. Frontiers in Immunology, 2020. **11**.
62. Atyeo, C.G., et al., *Maternal immune response and placental antibody transfer after COVID-19 vaccination across trimester and platforms*. Nature Communications, 2022. **13**(1): p. 3571.
63. Markov, P.V., et al., *The evolution of SARS-CoV-2*. Nature Reviews Microbiology, 2023. **21**(6): p. 361-379.

64. Chi, W.Y., et al., *COVID-19 vaccine update: vaccine effectiveness, SARS-CoV-2 variants, boosters, adverse effects, and immune correlates of protection*. J Biomed Sci, 2022. **29**(1): p. 82.
65. Huiberts, A.J., et al., *Effectiveness of Omicron XBB.1.5 vaccine against infection with SARS-CoV-2 Omicron XBB and JN.1 variants, prospective cohort study, the Netherlands, October 2023 to January 2024*. Euro Surveill, 2024. **29**(10).
66. Rubin, R., *As COVID-19 Cases Surge, Here's What to Know About JN.1, the Latest SARS-CoV-2 "Variant of Interest"*. Jama, 2024. **331**(5): p. 382-383.
67. Monto, A.S., A.S. Lauring, and E.T. Martin, *SARS-CoV-2 Vaccine Strain Selection: Guidance From Influenza*. J Infect Dis, 2022. **227**(1): p. 4-8.
68. Regev-Yochay, G., et al., *Correlates of protection against COVID-19 infection and intensity of symptomatic disease in vaccinated individuals exposed to SARS-CoV-2 in households in Israel (ICoFS): a prospective cohort study*. The Lancet Microbe, 2023. **4**(5): p. e309-e318.
69. Goldblatt, D., et al., *Correlates of protection against SARS-CoV-2 infection and COVID-19 disease*. Immunol Rev, 2022. **310**(1): p. 6-26.
70. Mahrokhian, S.H., et al., *COVID-19 vaccines: Immune correlates and clinical outcomes*. Hum Vaccin Immunother, 2024. **20**(1): p. 2324549.
71. Kent, S.J., et al., *Disentangling the relative importance of T cell responses in COVID-19: leading actors or supporting cast?* Nature Reviews Immunology, 2022. **22**(6): p. 387-397.
72. Yang, Y.J., et al., *Association of Gestational Age at Coronavirus Disease 2019 (COVID-19) Vaccination, History of Severe Acute Respiratory Syndrome Coronavirus 2 (SARS-CoV-2) Infection, and a Vaccine Booster Dose With Maternal and Umbilical Cord Antibody Levels at Delivery*. Obstetrics & Gynecology, 2022. **139**(3): p. 373-380.
73. Klein, S.L., P.S. Creisher, and I. Burd, *COVID-19 vaccine testing in pregnant females is necessary*. J Clin Invest, 2021. **131**(5).

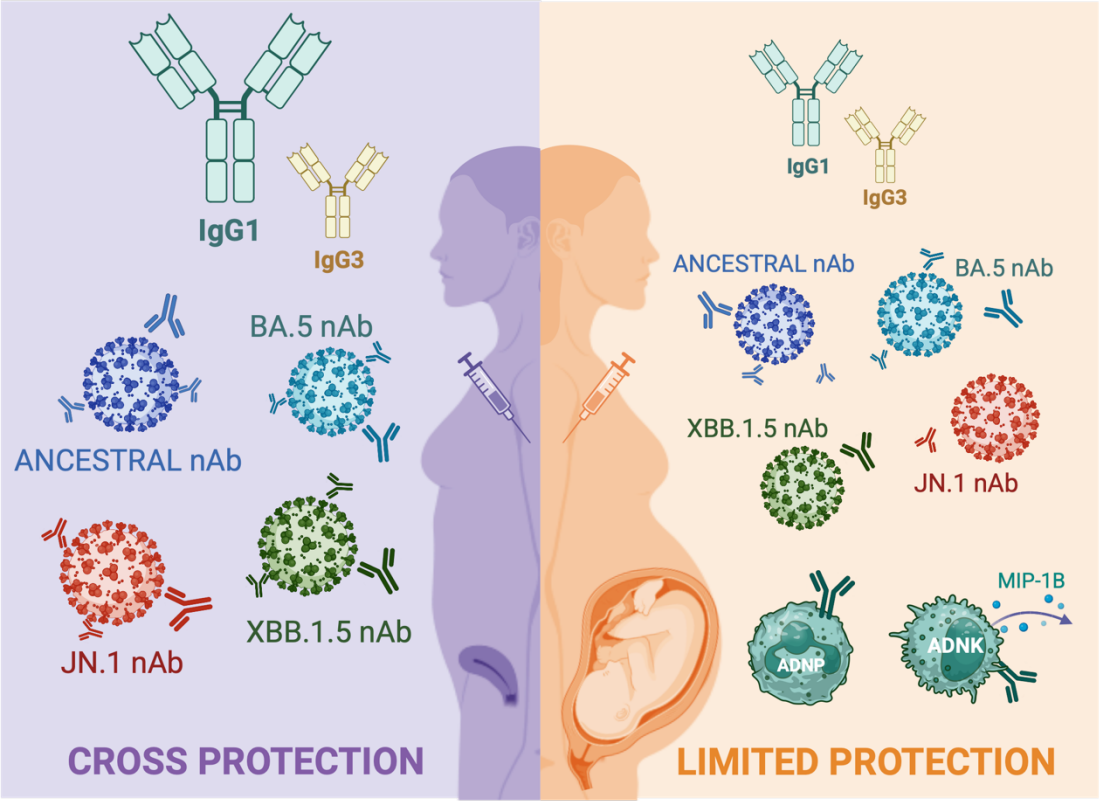

Graphical abstract

Table 1: Study Demographics

	Non-Pregnant n = 13	Pregnant n = 7	P-Value
Demographics	Mean ± SD	Mean ± SD	
Age	33.1 ± 6.1	32.9 ±3.2	0.93064
Vaccine Type			
Monovalent Booster	0 0%	2 28.5%	
Bivalent Booster	10 100%	5 71.5%	
Average Gestational Age (weeks)	-	22.4 ± 11.78	
	N %	**N %**	
Race			
White	8 61.5%	7 100%	
Black	2 15.4%	0 0%	
Asian	3 23.1%	0 0%	
Gestational Age (At Vaccination)	-	1st Trimester (n = 0) 0% 2nd Trimester (n = 6) 85.8% 3rd Trimester (n = 1) 14.2%	

Table 1.

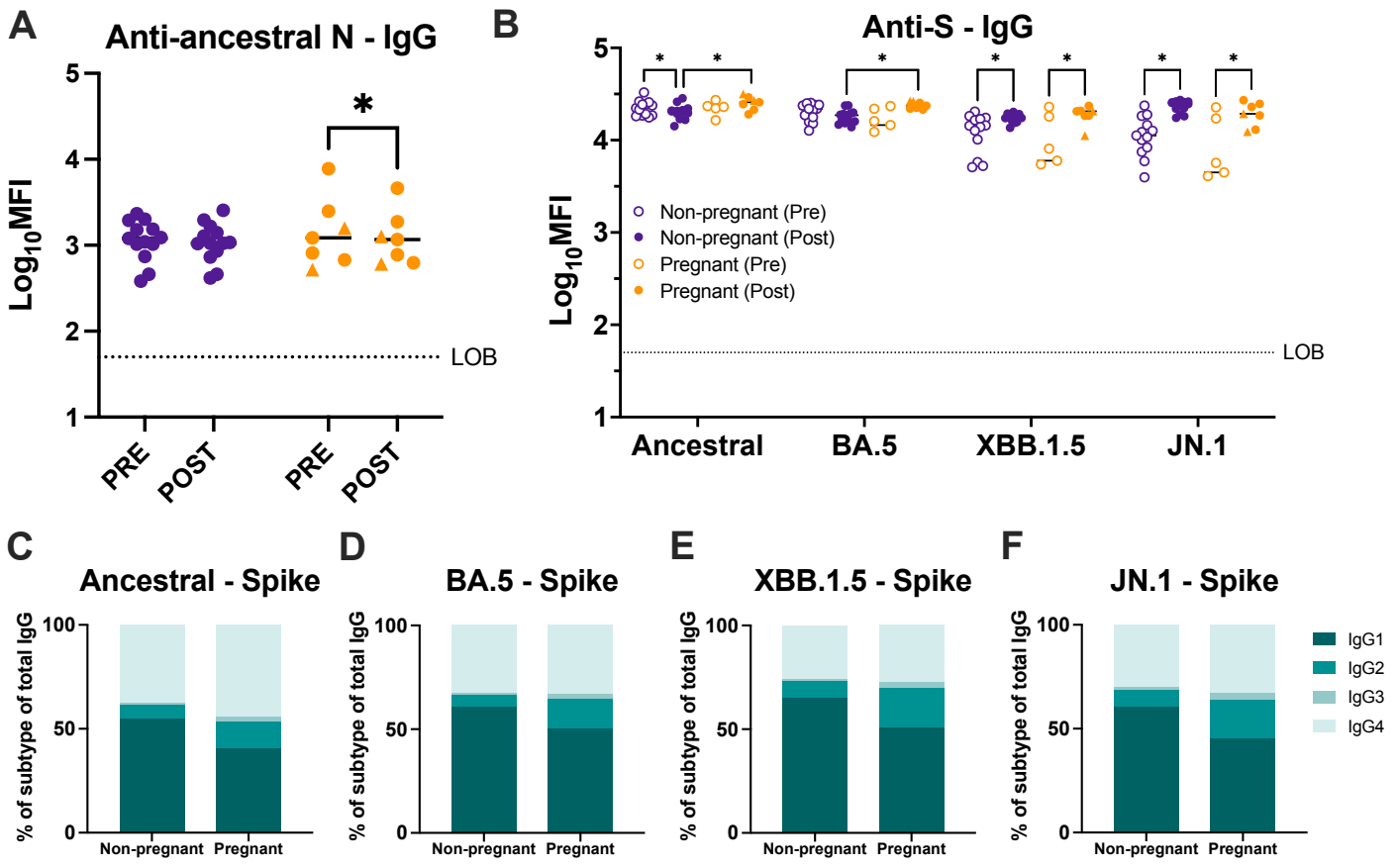

Figure 1. Vaccination differently induces IgG subtype responses during pregnancy. IgG antibody responses in serum pre and 3-5 weeks post-vaccination were measured by systems serology and reported as $\log_{10}$ mean fluorescence intensity (MFI). Pregnant women (n=7) are shown in orange and non-pregnant females (n=13) in purple. Triangles highlight women who received monovalent boosters and circles represent bivalent booster recipients. **(A)** Total IgG to ancestral nucleocapsid (N) protein**. (B)** Total IgG separated by SARS-CoV-2 vaccine (ancestral and BA.5) and variant (XBB1.5 and JN.1) spike (S) antigen and pregnancy status. **(C-F)** Relative abundance of IgG subtypes in pregnant and non-pregnant women as stacked bar plots representing each isotype as a percentage of Total IgG by **(C)** ancestral S, **(D)** BA.5 S, **(E)** XBB.1.5 S, and **(F)** JN.1 S. Data were analyzed by **(A)** repeated measures two-way ANOVA **(B-F)** linear mixed effects regression analysis with Bonferroni post-hoc. Asterisks indicate $p < 0.05$. Stippled line indicates limit of background (LOB) defined as the $\log_{10}$MFI of a defined negative control.

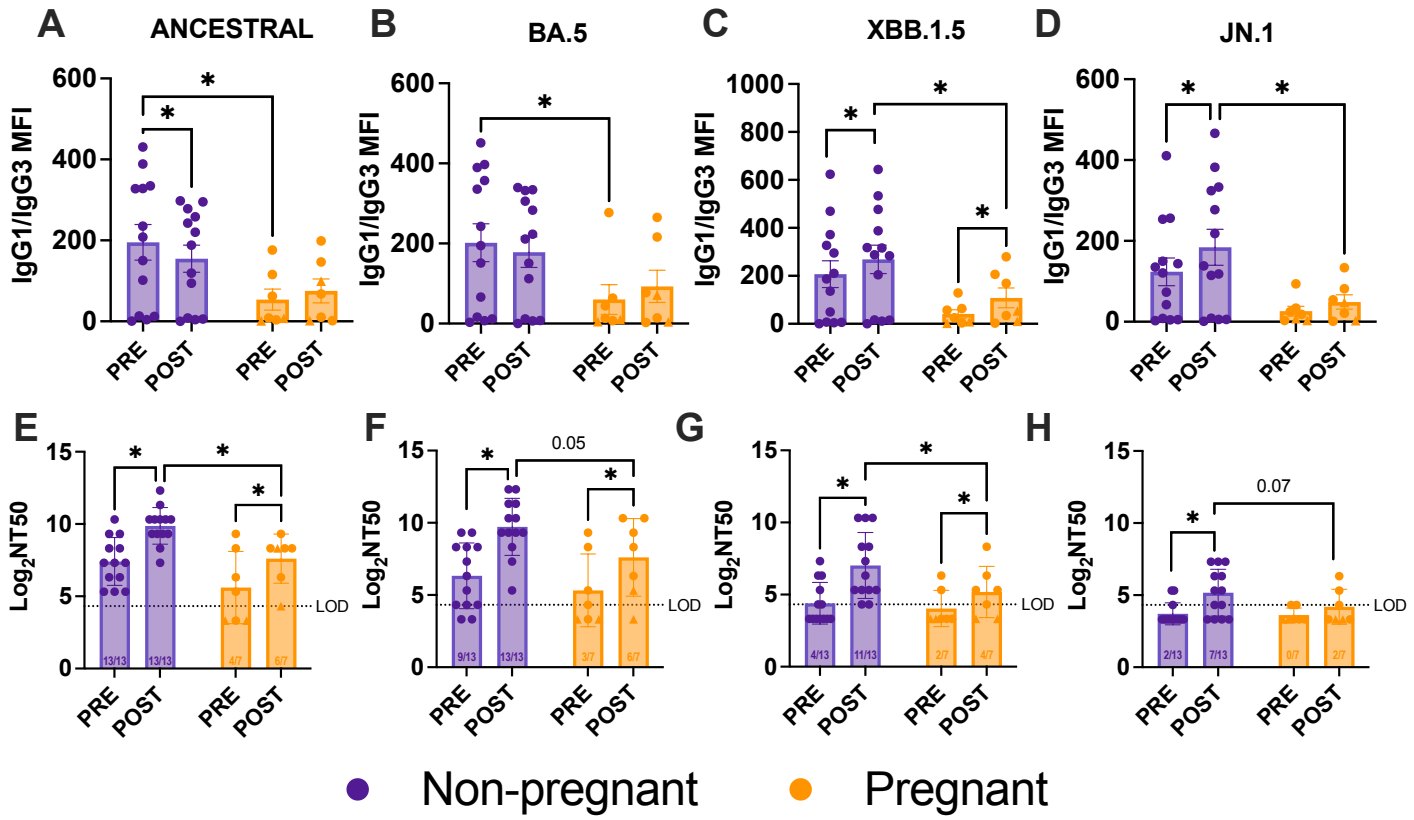

Figure 2. Pregnancy alters cross-neutralization of variants of concern. IgG antibody responses in serum pre and 3-5 weeks post-vaccination were measured by systems serology and reported as mean fluorescence intensity (MFI). Pregnant women (n=7) are shown in orange and non-pregnant females (n=13) in purple. Triangles highlight women who received monovalent boosters and circles represent bivalent booster recipients. **(A-E)** Ratio of IgG1:IgG3 antibodies specific to **(A)** ancestral spike (S), **(B)** BA.5 S, **(C)** XBB.1.5 S, and **(D)** JN.1 S. Neutralizing antibody (nAb) titers reported as Log_2 NT50 against live **(E)** ancestral, **(F)** BA.5, **(G)** XBB.1.5, and **(H)** JN.1 viruses. Ratios indicate number of women above the limit of detection (LOD) indicated by the stippled line. Data were analyzed by repeated measures two-way ANOVA with Bonferroni post-hoc. Asterisks indicate $p < 0.05$.

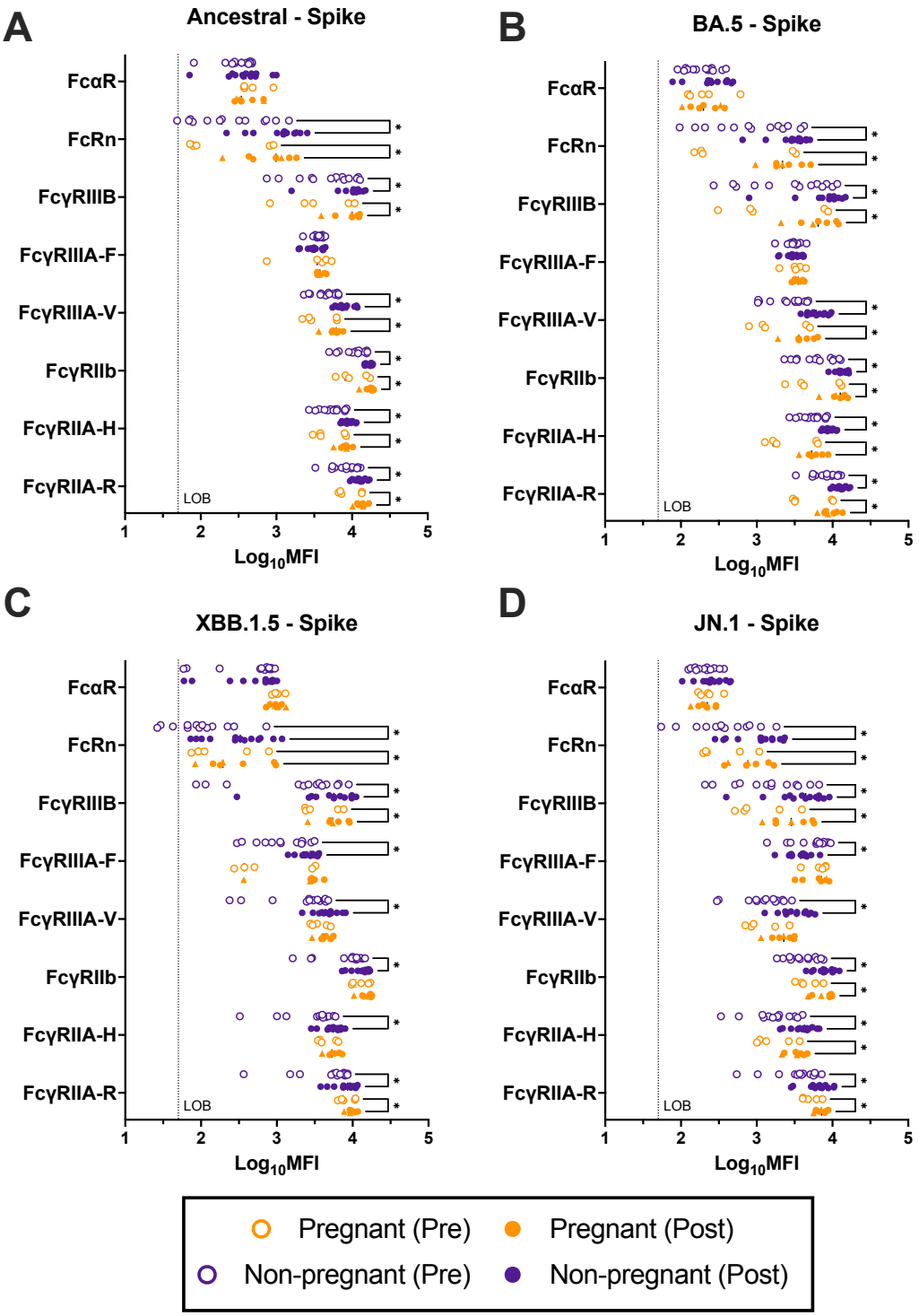

Figure 3. Fc receptor binding affinity is reduced in pregnant women in response to variants of concern. Serum antibody Fc receptor (FcR) binding affinity pre and 3-5 weeks post-vaccination were measured by multiplex Luminex bead assays and reported as $\log_{10}$ mean fluorescence intensity (MFI). Pregnant women (n=7) are shown in orange and non-pregnant females (n=13) in purple. Triangles highlight women who received monovalent boosters and circles represent bivalent booster recipients. Affinity for FcγRIIA-R, FcγRIIA-H, FcγRIIb, FcγRIIIA-V, FcγRIIIA-F, FcγRIIIB, FcRn, and FcαR was determined for **(A)** ancestral spike (S), **(B)** BA.5 S, **(C)** XBB.1.5 S, and **(D)** JN.1 S. Data were analyzed by linear mixed effects regression analysis with Bonferroni post-hoc. Asterisks indicate $p < 0.05$. Stippled line indicates limit of background (LOB) defined as the $\log_{10}$MFI of a defined negative control.

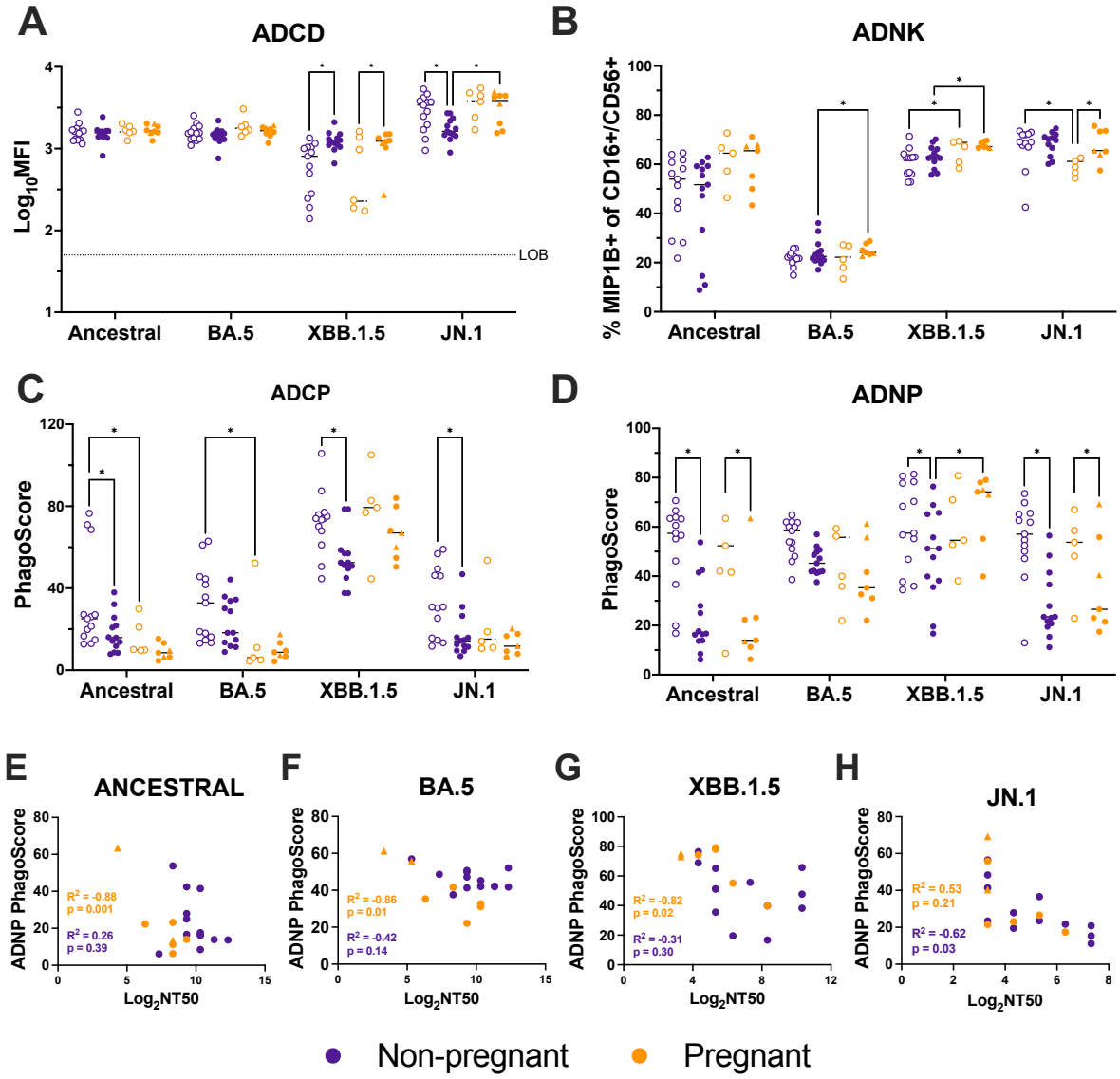

Figure 4. Non-neutralizing and neutralizing antibody functions are negatively correlated among pregnant women. Non-neutralizing antibody functions were measured pre and 3-5 weeks post-vaccination. Pregnant women (n=7) are shown in orange and non-pregnant females (n=13) in purple. Triangles highlight women who received monovalent boosters and circles represent bivalent booster recipients. **(A)** antibody dependent complement deposition (ADCD) was measured by assessing antibody affinity for C3 protein and is reported as $\log_{10}$ mean fluorescence intensity (MFI). Stippled line indicates limit of background (LOB) defined as the $\log_{10}$MFI of a defined negative control. NK cells isolated from donor blood were utilized to assess **(B)** antibody dependent NK cell cytotoxicity (ADNK), or the ability of antigen specific serum antibody to include NK cell cytokine production or degranulation. Data are reported as % MIP1B+ cells of CD16+/CD56+ NK cells. **(C)** THP-1 monocyte cell line was used to measure antibody dependent cellular phagocytosis (ADCP), or the ability of antibody to induce phagocytosis of antigen. **(D)** Neutrophils isolated from donor blood were used to measure antibody dependent neutrophil phagocytosis (ADNP), or the ability of antibody to induce neutrophil phagocytosis of antigen. ADCP and ADNP are reported as a PhagoScore, calculated as (% bead positive monocytes/neutrophils) * (geometric MFI of each cell). **(E-H)** Pearson correlations between neutralizing antibody titers (Log_2NT50) and ADNP PhagoScores for are shown for: **(E)** ancestral, **(F)** BA.5, **(G)** XBB.1.5, and **(H)** JN.1 viruses. Separate R2 and p-values are shown for each virus separated by pregnancy status. **(A-E)** Data were analyzed by linear mixed effects regression analysis with Bonferroni post-hoc. Asterisks indicate $p < 0.05$.

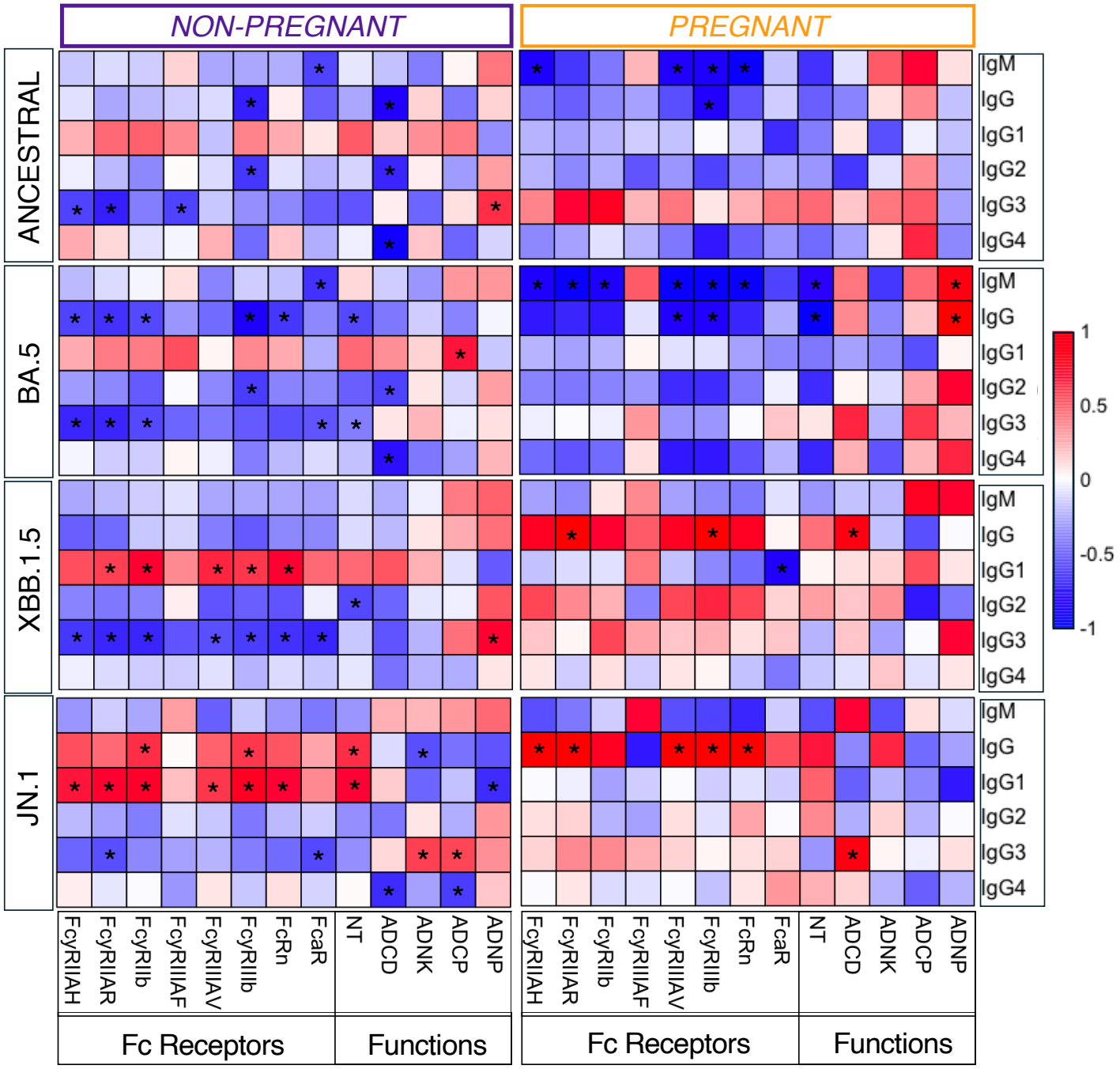

Figure 5. Correlations among IgG subclasses and antibody functional phenotypes differ between pregnant and nonpregnant women. Post-vaccination systems serology measures including isotype subclasses, FcR affinity, non-neutralizing functions, and neutralizing antibody (nAb) titers were $\log_{10}$ transformed and used for Spearman correlation analyses. Isotypes (y-axis) were correlated with functional measures (x-axis). Analyses were performed by pregnancy status. Asterisks indicate $p < 0.05$.

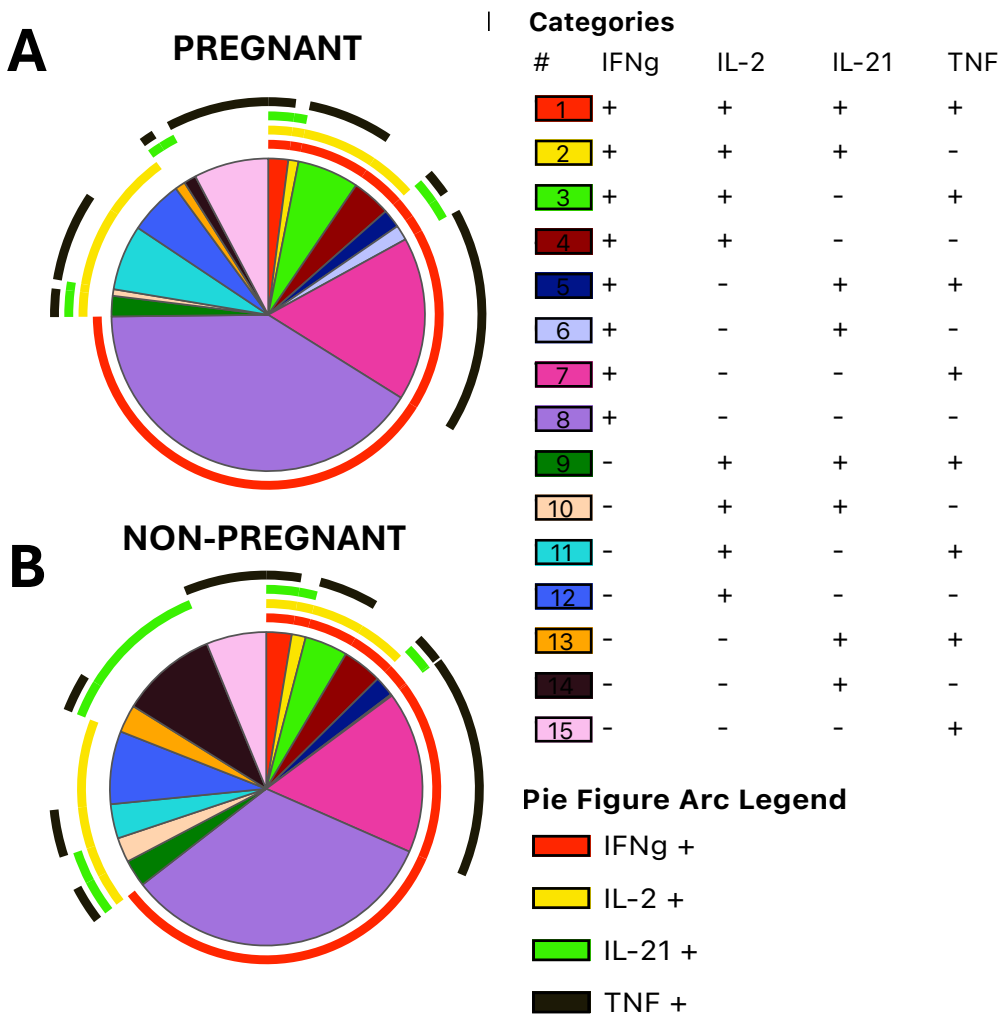

Figure 6. CD4+ T cells have reduced polyfunctionality among pregnant women. Peripheral blood mononuclear cells (PBMCs) were collected pre and 3-5 weeks post-vaccination for flow cytometry analyses. Cytokine-producing, antigen-specific CD4+T cells for **(A)** pregnant (n=7) and **(B)** non-pregnant (n=3) women represented in pie charts broken down by the 15 cytokine combination categories. Arcs identify slices of the pie that express each specific cytokine**.** R values are shown for each correlation, and asterisks indicate $p < 0.05$.

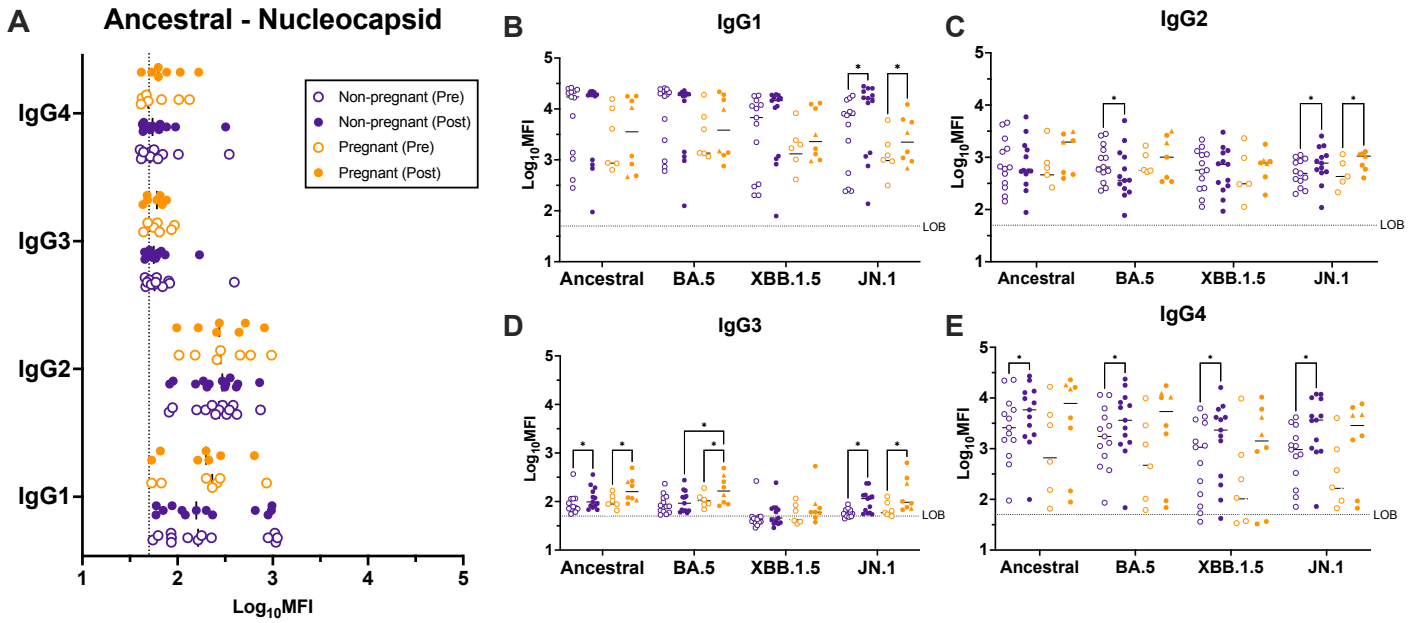

Supplemental Figure 1. Vaccination differently induces IgG subtype responses during pregnancy. IgG antibody responses in serum pre and 3-5 weeks post-vaccination were measured by systems serology and reported as $\log_{10}$ mean fluorescence intensity (MFI). Pregnant women (n=7) are shown in orange and non-pregnant females (n=13) in purple. Triangles highlight women who received monovalent boosters and circles represent bivalent booster recipients. **(A)** IgG subtype abundance to ancestral nucleocapsid (N) protein**.** IgG subtypes, including **(B)** IgG1 **(C)** IgG2, **(D)** IgG3, and **(E)** IgG4, in response to ancestral, BA.5, XBB.1.5, and JN.1 spike protein. Data were analyzed by linear mixed effects regression analysis with Bonferroni post-hoc. Asterisks indicate $p < 0.05$.

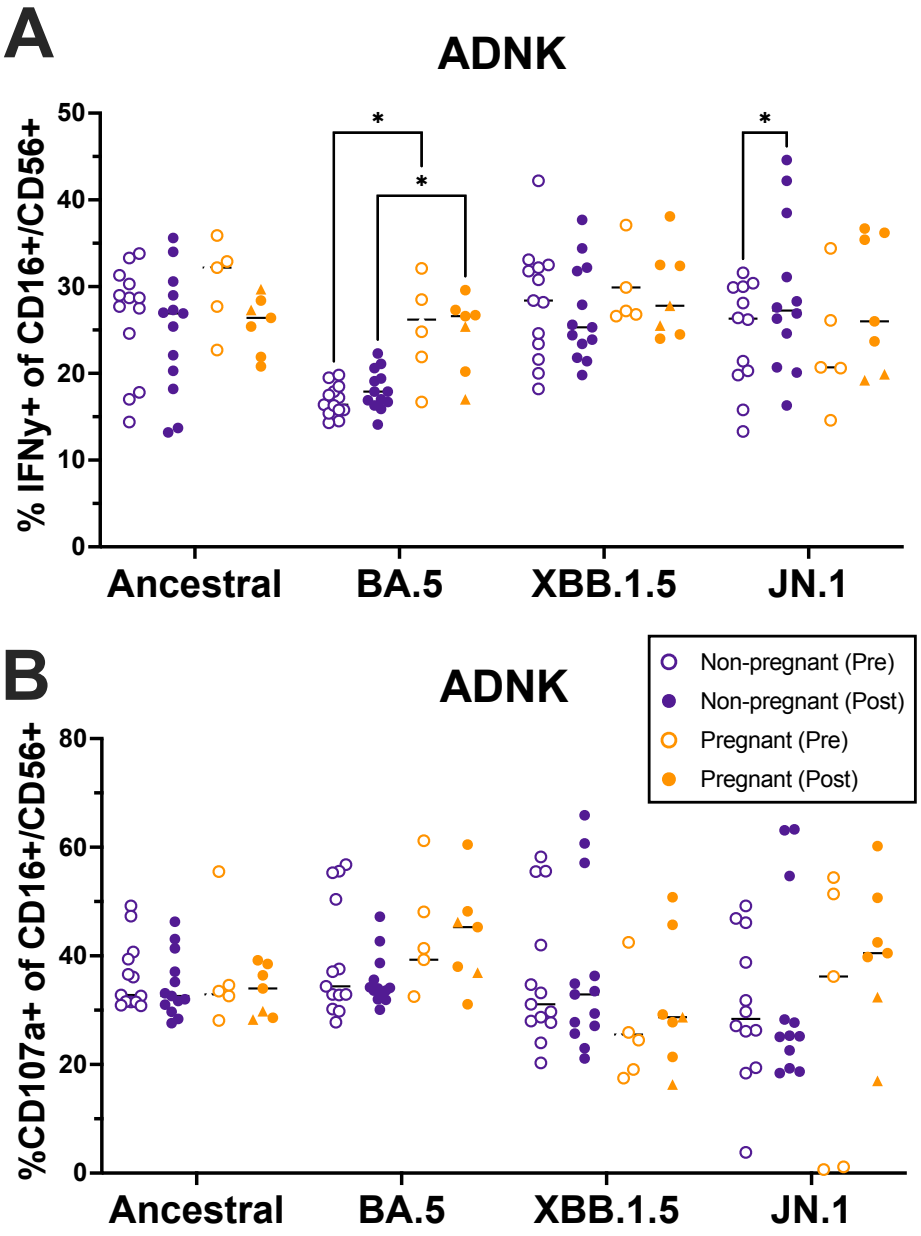

Supplemental Figure 2. Additional antibody-dependent NK cell responses by pregnancy status. NK cells isolated from donor blood were utilized to assess antibody dependent NK cell cytotoxicity (ADNK), or the ability of antigen specific serum antibody to include NK cell cytokine production or degranulation in serum pre and 3-5 weeks post-vaccination. Pregnant women (n=7) are shown in orange and non-pregnant females (n=13) in purple. Triangles highlight women who received monovalent boosters and circles represent bivalent booster recipients. ADNK was measured as ability to induce **(A)** IFNy production or **(B)** NK cell degranulation, as measured by CD107a positivity. Data were analyzed by linear mixed effects regression analysis with Bonferroni post-hoc. Asterisks indicate $p < 0.05$.

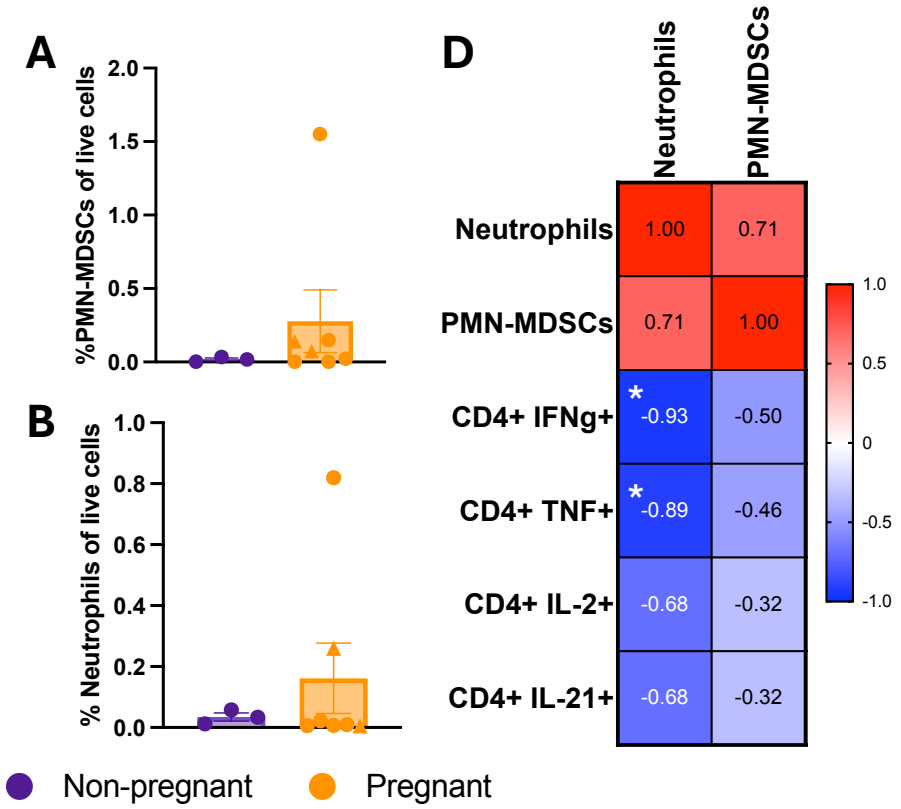

Supplemental Figure 3. Polymorphonuclear myeloid-derived suppressor cells correlate with CD4+ cytokine producing cells. Peripheral blood mononuclear cells (PBMCs) were collected pre and 3-5 weeks post-vaccination for flow cytometry analyses. Pregnant women (n=7) are shown in orange and non-pregnant females (n=3) in purple. Triangles highlight women who received monovalent boosters and circles represent bivalent booster recipients. **(A)** Neutrophils and **(C)** polymorphonuclear myeloid-derived suppressor cells (PMN-MDSCs) were quantified by flow cytometry and reported as a percentage of total live single cells. **(D)** Pearson correlations between cytokine producing CD4+ T cells, neutrophils, and PMN-MDSCs from pregnant women. R values are shown for each correlation, and asterisks indicate $p < 0.05$.

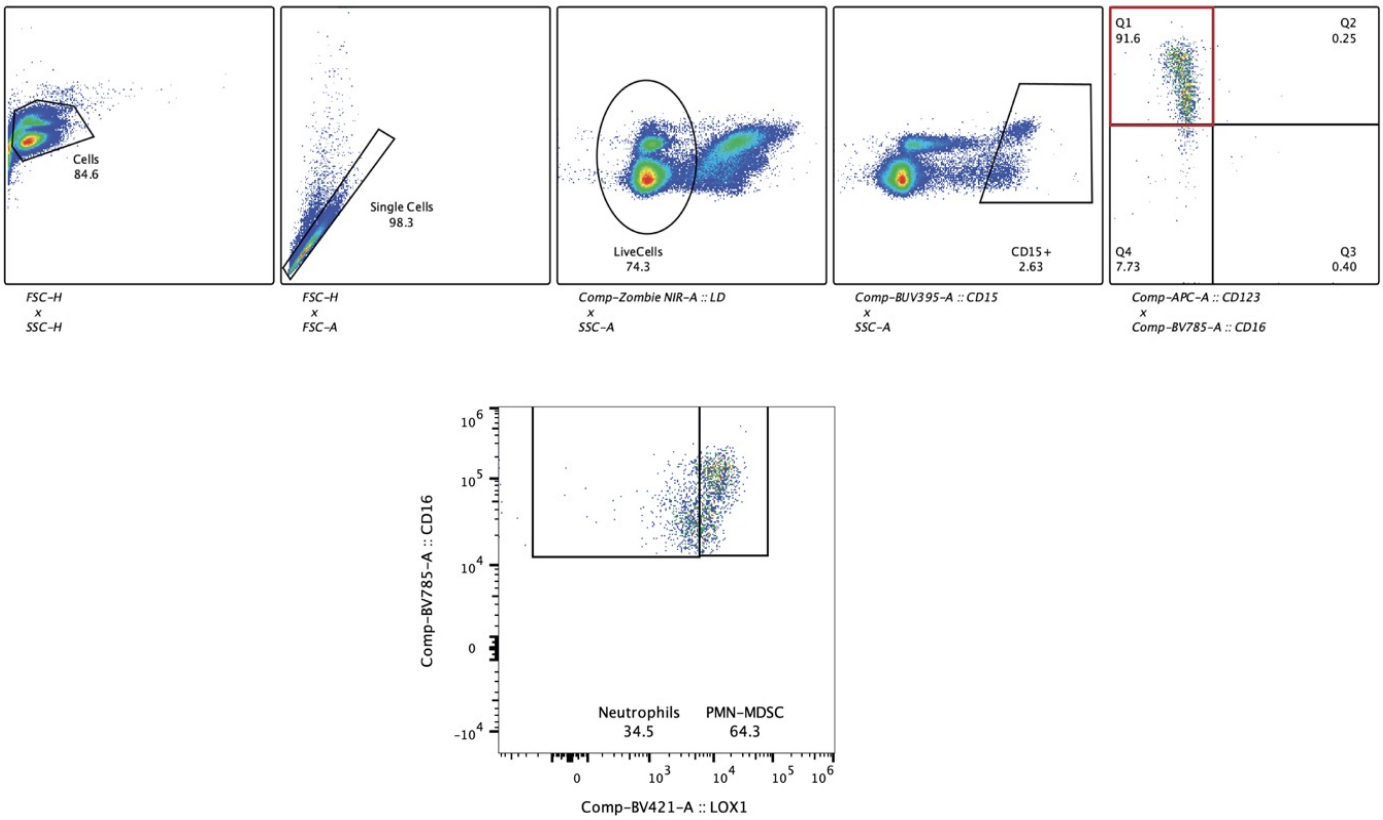

Supplemental Figure 4. PMN-MDSC gating strategy.

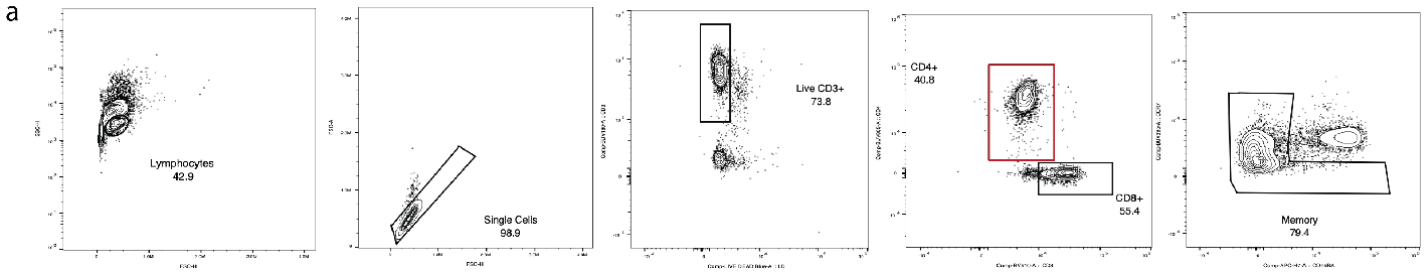

Supplemental Figure 5. Cytokine positive CD4+ T cells.

Supplemental Table 1A-B. Broad immune cell phenotyping (BIP) flow cytometry panel. (A) surface staining markers and **(B)** intracellular markers.

A. Surface

Fluorophore	Marker	Clone	Catalog	Vendor
BV570	CD33	WM53	303417	BioLegend
BV480	CD11c	B-ly6	566135	BD Biosciences
APC	CD123	6H6	306012	BioLegend
BV510	CD25	M-A251	563352	BD Biosciences
BV650	CCR7	G043H7	353234	BioLegend
BV421	LOX1	15C4	358610	BioLegend
BV711	CD38	HIT2	563965	BD Biosciences
APC-Cy7	CD19	SJ25C1	363010	BioLegend
APC-Cy7	CD56	5.1H11	362512	BioLegend
BV750	HLA-DR	L243	307672	BioLegend
BUV661	CD3	UCHT1	612964	BD Biosciences
BUV496	CD4	SK3	612936	BD Biosciences
BUV737	CD8	SK1	612754	BD Biosciences
BV785	CD16	3G8	302046	BioLegend
BUV805	CD14	M5E2	612902	BD Biosciences
BV605	CD86	BU63	374214	BioLegend
BUV563	CD45RA	HI100	612926	BD Biosciences
BUV395	CD15	H198	563872	BD Biosciences
Spark NIR	CD27	O232	302856	BioLegend
PE-Cy5	CD21	B-ly4	551064	BD Biosciences
PE-Cy5.5*	CD138	MI15	356502	BioLegend
PE-CF594	KLRG1	2F1	565393	BD Biosciences
BB790	IgD	IA6-2	BD Custom	BD Biosciences
BUV615	PD-1	EH12.1	612991	BD Biosciences

B. Intracellular

Fluorophore	Marker	Clone	Catalog	Vendor
Pacific Blue	FOXP3	206D	320116	BioLegend
PE-Cy7	Ki-67	Ki-67	350526	BioLegend
Alexa Fluor 488	CPT1a	8F6AE9	ab171449	Abcam
Alexa Fluor 680**	HK2	EPR20839	ab228819	Abcam
Alexa Fluor 532***	VDAC1	20B12AF2	ab14734	Abcam

Alexa Fluor 405	Tomm20	EPR15581-54	ab210047	Abcam
Alexa Fluor 647	GLUT1	EPR3915	ab195020	Abcam

Notes: * conjugated using PE/Cy5.5 Conjugation Kit - Lightning-Link (ab102899)

** conjugated using DyLight 680 Conjugation Kit (Fast) - Lightning-Link (ab201804)

*** conjugated using Alexa Fluor 532 Antibody Labeling Kit (Thermo Fisher, A20182)

Supplemental Table 2. Intracellular cytokine staining (ICS) flow cytometry panel. (A) surface staining markers and **(B)** intracellular markers.

A. Surface

Fluorophore	Marker	Clone	Catalog	Vendor
BUV395	CCR7	2-L1-A	749655	BD Biosciences
BV650	CXCR3	1C6	740603	BD Biosciences
PE CF594	KLRG1	2F1	565393	BD Biosciences
BV605	CD69	FN50	562989	BD Biosciences
BUV563	CD25	2A3	612918	BD Biosciences
BUV661	PD-1	EH12.1	750260	BD Biosciences
BUV737	TIM-3	7D3	748820	BD Biosciences
BV570	CD28	CD28.2	302926	Biolegend
PE Cy5	CD127	HIL-7R-M21	BD Custom	BD Biosciences
BUV805	CD4	SK3	612887	BD Biosciences
APC H7	CD45RA	HI100	560674	BD Biosciences
BB660	Tigit	741182	BD Custom	BD Biosciences
BV711	OX40	ACT35	563664	BD Biosciences
BV786	CD27	L128	563327	BD Biosciences
PE Cy7	CTLA-4	BNI3	BD Custom	BD Biosciences
BV510	CD8a	HIT8a	300934	Biolegend
BB790	CXCR5	RF8B2	BD Custom	BD Biosciences

B. Intracellular

Fluorophore	Marker	Clone	Catalog	Vendor
PE	IL-21	3A3-N2	513004	BioLegend
AF680**	HK2	EPR20839	ab228819	Abcam
AF488	TCF1	812145	IC8224G	FisherScientific
BV421	IL-2	MQ1-17H12	564164	BD Biosciences
AF532***	VDAC1	20B12AF2	ab14734	Abcam

BV750	TNF	MAb11	566359	BD Biosciences
PECy5.5*	CPT1a	8F6AE9	ab128568	Abcam
AF405	Tomm20	EPR15581-54	ab210047	Abcam
Alexa647	GLUT1	EPR3915	ab195020	Abcam
BUV496	CD3	UCHT1	612940	BD Biosciences
BB700	IFNy	B27	566394	BD Biosciences

Notes: * conjugated using PE/Cy5.5 Conjugation Kit - Lightning-Link (ab102899)

** conjugated using DyLight 680 Conjugation Kit (Fast) - Lightning-Link (ab201804)

*** conjugated using Alexa Fluor 532 Antibody Labeling Kit (Thermo Fisher, A20182)